Stabilizing by Periodic Driving

LIM FU KANG

(A0086950W)

Department of Physics

National University of Singapore

Supervisor: Assoc. Prof Gong Jiang Bin

Co-Supervisor: Dr. Wang Qinghai

A thesis submitted in partial fulfillment of the requirements for the degree of

Bachelor of Science with Honours in Physics

AY2014/2015

Acknowledgement

First of all, I would like to express my gratitude to Associate Prof. Gong Jiangbin for offering this project to me, guiding me along the project by clarifying my never ending doubts and helping me patiently whenever I met up with problems. Furthermore, with the high expectations that he set for me regarding this project, he inspired me to have even more interest about quantum mechanics, allowing me to reach an even higher level of understanding in this amazing field.

Secondly, I would also like to express my gratitude to my co-supervisor Dr. Wang Qinghai who had also helped me in preparation of manuscripts, guidance in teaching me Mathematica and understanding of this project. In addition to that, I am also truly grateful for him who had inspired and hence built a strong foundation of physics in me since year 1 of my undergraduate study in NUS.

Last but not least, I would also like to take this opportunity to thank my parents, brother and Jessica who had given me a lot of support throughout the course of my entire undergraduate study in NUS. I would also like to thank Shannon, Pamelyn and Livia for the wonderful friendship and support given to me throughout my undergraduate study.

I am truly grateful for all the support and inspirations that all of you had given me and will my best in everything I do in the future.

Abstract

In general, it is expected that the time evolution of a system described by a time-dependent, non-Hermitian Hamiltonian, to be unstable with exponential growth or decay. However, in depth studies of such systems by Gong. and Wang. [5] and Yogesh et. al. [39] discovered that the dynamics of these unique systems can be stabilized via the use of a periodic driving field. This can be achieved because by driving the system with a periodic field, there is a possibility that all the eigenphases of the associated Floquet operator become real. In this thesis, a thorough study of periodic driving of such systems will be described and explained. In addition, it will also be shown that stabilization of such system is still possible via the use of periodic driving even though when a system's parameter (e.g. energy difference of a qubit system) is being varied. Furthermore, a detailed comparison of 2 different methods to study the problem will also be presented to illustrate the pros and cons of tackling the problem using each method. Lastly, some of the applications derived from this study will also be described to emphasize the usefulness of this study and to inspire more detailed research to be done in the future.

Contents

List of Figures

Chapter 1

Introduction

Quantum mechanics is a general theory. The basic formalisms of quantum mechanics are being introduced to physicists during their undergraduate studies as postulates to study the theory. Idealized toy models are also being utilized to enable simplified calculations to be performed, thereby arousing interest in learning more about the subject.

However, in real experimental settings, such idealized models are not sufficient to describe physical phenomenon accurately. Remodeling them to describe the situation more accurately and performing more complicated calculations are thus essential aspects of training for a physicist. In addition to acquiring remodeling skills, it is always interesting to question the basic formalism of quantum mechanics again and appreciate the reasons why they become important postulates widely accepted today. In doing so, it will help us attain a higher level of understanding about the theory.

Inspired by the above, this thesis is being written for 2 purposes: First, we understand the fundamental postulates of quantum mechanics and second, we aim to study a realistic model to describe a periodically driven open system. In the first part of the thesis, the postulate that the Hamiltonian of a system is always Hermitian (According to postulate 2 in chapter 1) is being questioned. This is because, by having a Hermitian Hamiltonian to describe a system, it guarantees that the energy eigenspectrums are definitely real (according to linear algebra). This also makes logical sense because the energies that we measured are also real numbers and not imaginary numbers. However, in certain physical situations the use of non-Hermitian Hamiltonians to describe the physical situation becomes necessary such as the case of describing dissipative systems [1,16]. This field of study is interesting because it had been discovered that some non-Hermitian Hamiltonians also gave rise to real energy eigenspectrum (e.g. Non-Hermitian Hamiltonians that obey PT-symmetry) [3,31-36]. Therefore, it inspired us to reflect upon this postulate and question whether it is just a subset of an even more general postulate. Upon reading up on more literatures, it is discovered that for an operator to have a real spectrum of eigenvalues, the condition that it must be Hermitian is not absolutely necessary [1,16]. This is observed especially in the case of a type of symmetry known as the Parity-Time symmetry (PT

symmetry) whereby one can still obtain a real set of eigenvalues for non-Hermitian operators [3,4,6-13].

Motivated by the questioning of this postulate, we became interested in studying time-dependent non-Hermitian systems and researched on stabilizing the time evolution of such systems via the use of periodic driving [5]. Stabilization of such system is possible because, the eigenphases of the associated Floquet operator might become all real when the system is periodically driven [5]. The study on these systems is rather new in the field because most literatures to date are studying on time-independent systems [14-20] whereas in our study, we are studying on time-dependent systems.

Lastly, this study is of great interest to us because it can also be used to map the stability of a driven non-Hermitian Rabi model into a band structure problem of a class of lattice Hamiltonians [5]. Furthermore, the realm of optics [21-24] also provided a way to conduct experiments on this theoretical research to motivate further and deeper understanding on this interesting area of quantum mechanics.

Chapter 2

Some Basic Quantum Mechanics

2.1 Postulates of Quantum Mechanics

Quantum Mechanics is a theory that is being formalized based on a number of postulates which comes from a plethora range of experimental observations [25]. Being postulates that are solely attained via experimental observations, they are so fundamental that it cannot be derived from first principles. Instead, they are taken as an initial set of rules for physicists to develop further on the theory of quantum mechanics. Generally, the following are the 5 postulates that are most commonly quoted [25] in various introductory quantum mechanics textbooks:

Postulate 1: The state of a quantum mechanics system is completely described by a wave function, $|\Psi(x,t)\rangle$ in the Hilbert space.

Postulate 2: For every measurable observable, A of the system there exists a corresponding Hermitian operator, A whose eigenvectors form a complete basis.

Postulate 3: For any measurement involving an observable corresponding to an operator, A the only values that will be measured will be the eigenvalues, a_n of the operator.

$$A|\psi_n\rangle = a_n|\psi_n\rangle \tag{2.1}$$

where $|\psi_n\rangle$ is the *n*th eigenstate of the operator, A.

Postulate 4: If the system is in a state described by a wave function and the value of the observable, A is measured once each on many identically prepared systems, the average value of all the measurements will be:

$$\langle A\rangle = \frac{\int_{-\infty}^{\infty}\Psi^*(x)\mathrm{A}\Psi(x)dx}{\int_{-\infty}^{\infty}\Psi^*(x)\Psi(x)dx} = \int_{-\infty}^{\infty}\Psi^*(x)A\Psi(x)\,dx \tag{2.2}$$

Postulate 5: The time evolution of the state vector of a closed system is unitary (reversible) and is being governed by the time-dependent Schrödinger equation:

$$i\hbar\frac{\partial}{\partial t}|\Psi(x,\mathrm{t})\rangle = H|\Psi(x,t)\rangle \tag{2.3}$$

Hence from the above postulates, we can group them into 2 different categories whereby the first 4 of them actually describes the quantum mechanical system at a given time, whereas the last postulate describes how the system evolves in time.

For the purpose of this thesis, we will focus on the last postulate because time-dependent Hamiltonians are being studied in the thesis and we will need a strong foundation to be established before we can proceed further.

2.2 The Time Evolution Operator, $U(t, t_0)$

In this section, the Hamiltonian, H discussed will be Hermitian for the reader to have a better understanding of the more fundamental mathematical formalism of quantum mechanics before going deeper into the theory.

To begin with, we start by trying to find out how a quantum system evolves in time. In other words, it means that if we are given an initial state, $|\Psi(t_0)\rangle$ at time, t_0, what will happen to the state after some time, t later? Since we usually associate an operator to an observable in quantum mechanics, we shall adopt a similar method by introducing a linear time evolution operator or propagator, $U(t, t_0)$ to relate the initial state, $|\Psi(t_0)\rangle$ to the final state, $|\Psi(t)\rangle$ as shown in equation (2.4):

$$|\Psi(t)\rangle = U(t, t_0)|\Psi(t_0)\rangle \tag{2.4}$$

Therefore, we can treat $U(t, t_0)$ as an operator that propagates a state with respect to time and hence given the name: time propagator.

Additionally, from equation (2.4), it can also be easily inferred physically that the time propagator is an identity operator when $t = t_0$ as shown in equation (2.5) because no time is given for the system to evolve at all.

$$U(t_0, t_0) = I \tag{2.5}$$

where I is the unit (Identity) operator. In other words, the final state must be the same as the initial state if no time is being allowed for evolution.

Given all the above, our main aim is to find out the mathematical expression of the time evolution operator, $U(t, t_0)$. In order to do so, a substitution of equation (2.4) into equation (2.3) is being performed and the derivation is being shown below:

$$i\hbar \frac{\partial}{\partial t}[U(t, t_0)|\Psi(t_0)\rangle] = H(t)U(t, t_0)|\Psi(t_0)\rangle$$

$$\frac{\partial U(t, t_0)}{\partial t}\Big|\Psi(t_0)\rangle = -\frac{i}{\hbar}H(t)U(t, t_0)\Big|\Psi(t_0)\rangle$$

$$\frac{\partial U(t, t_0)}{\partial t} = -\frac{i}{\hbar}H(t)U(t, t_0) \tag{2.6}$$

In general, the solution of equation (2.6) depends on whether the Hamiltonian, H is time-dependent or not [25]. When the Hamiltonian is time-dependent, we get the following solution shown in equation (2.7) for $U(t, t_0)$ in the Schrödinger picture.

$$U_S(t, t_0) = \boldsymbol{T}exp\left[-\frac{i}{\hbar}\int_{t_0}^{t} H(t')dt'\right] \tag{2.7}$$

where $\boldsymbol{T}$ is the Time-ordering operator, also known as the Dyson's Series.

As for the case where the Hamiltonian is time-independent, we get the following expression for $U(t, t_0)$ as shown in equation (2.8).

$$U(t, t_0) = \exp\left[-\frac{i}{\hbar}H(t - t_0)\right] \tag{2.8}$$

From equation (2.8), the time evolution operator, $U(t, t_0)$ can be easily shown to be unitary according to the following short mathematical proof.

Proof

$$U^{\dagger}(t, t_0)U(t, t_0) = \exp\left[\frac{i}{\hbar}H^{\dagger}(t - t_0)\right] \cdot \exp\left[-\frac{i}{\hbar}H(t - t_0)\right]$$

$$= \exp\left[\frac{i}{\hbar}H(t - t_0)\right] \cdot \exp\left[-\frac{i}{\hbar}H(t - t_0)\right]$$

$$= I \qquad \text{(QED)}$$

Nonetheless, for the case of a time-dependent Hamiltonian, the time evolution operator, $U(t, t_0)$ is also unitary as well and can be shown with a short mathematical proof as follow:

Proof

Suppose we substitute equation (2.4) into the time-dependent Schrödinger equation

equation (2.3), we get the following expression and its complex conjugate,

$$\frac{dU(t,t_0)}{dt} = -\frac{i}{\hbar}H(t)U(t,t_0) \qquad \text{and} \qquad \frac{dU^\dagger(t,t_0)}{dt} = \frac{i}{\hbar}U^\dagger(t,t_0)H^\dagger(t)$$

At $t = t_0$, $U(t,t_0) = I$. Therefore, $U^\dagger(t_0,t_0)U(t_0,t_0) = I$, and we say that $U(t,t_0)$ is unitary at $t = t_0$.

To prove for all time, t, we make use of the product rule as follow:

$$\begin{aligned}\frac{d}{dt}\Big(U^\dagger(t,t_0)U(t,t_0)\Big) &= \left(\frac{dU^\dagger(t,t_0)}{dt}\right)U(t,t_0) + U^\dagger(t,t_0)\left(\frac{dU(t,t_0)}{dt}\right)\\ &= \left(\frac{i}{\hbar}U^\dagger(t,t_0)H^\dagger(t)\right)U(t,t_0) + U^\dagger(t,t_0)\left(-\frac{i}{\hbar}H(t)U(t,t_0)\right)\\ &= \frac{i}{\hbar}U^\dagger(t,t_0)\Big(H^\dagger(t) - H(t)\Big)U(t,t_0)\\ &= 0 \qquad \text{(QED)}\end{aligned}$$

Thus, we had succeeded in proving that $U^\dagger(t,t_0)U(t,t_0) = I$ at all times, t and thereby conclude that $U(t,t_0)$ is a unitary operator as long as the Hamiltonian is Hermitian i.e. $H^\dagger(t) = H(t)$.

In summary, the time evolution operator for both a time-independent Hermitian Hamiltonian and a time-dependent Hermitian Hamiltonian are unitary.

This unitarity condition of the time evolution operator, $U(t,t_0)$ in a closed system is in fact very important in physics because when this is fulfilled, it preserves the normalization of the state kets. In other words, if the initial state $|\Psi(t_0)\rangle$ is being normalized at t_0, it should still remain normalized at some time, t later. The following proof will show the mathematical importance for the need of $U(t,t_0)$ to be unitary.

Proof

Suppose the norm of the state of the system is at unity at any arbitrary time, t, (i.e. $\langle\Psi(t)|\Psi(t)\rangle = 1$) we can substitute equation (2.4) into the expression and obtain the following statement:

$$\langle\Psi(t)|\Psi(t)\rangle = \big\langle\Psi(t_0)\big|U^\dagger(t,t_0)|U(t,t_0)\big|\Psi(t_0)\big\rangle = 1$$

For this statement to hold, the unitarity condition of the time evolution operator, $U(t,t_0)$ as stated in equation (2.9) must be fulfilled.

$$U^\dagger(t,t_0)U(t,t_0) = I \qquad (2.9)$$

Once equation (2.9) is being fulfilled, it guarantees that $\langle\Psi(t_0)|\Psi(t_0)\rangle = 1$ is true and since t is any arbitrary time, we can conclude that there probability is being conserved when the time evolution operator is unitary.

(QED)

With this, we see that the unitarity of the evolution operator actually helps ensure that probability is being conserved. This is in fact an important concept that will be emphasized for the rest of the chapters when dealing with non-Hermitian time dependent Hamiltonians in which a more general mathematical approach is being devised to tackle them.

Lastly, on a side note, the time evolution operator also satisfy the composition property [25,26] which means that to evolve the state from t_0 to t_2, we can consider evolving the system from t_0 to t_1 and then evolve the state obtained from t_1 to t_2, whereby $t_0 < t_1 < t_2$. This is being illustrated mathematically in equation (2.10) below.

$$U(t_2, t_0) = U(t_2, t_1)U(t_1, t_0) \tag{2.10}$$

In summary, with the above postulates and a basic understanding of the time evolution operator, we are now ready to go on further and understand more complicated evolution of a quantum system.

Chapter 3

Periodically Driven Systems

In this chapter, periodically driven systems will be discussed with the use of Hermitian Hamiltonian for the reader to familiarize with the fundamental picture first before going into more general ideas in later chapters. The essence of this study is to mathematically describe the oscillation of the population of a system known as the Rabi oscillation. With the observation of a coherent and periodic population oscillation, it helps in concluding that the stabilization of a system is being achieved in a periodic field.

3.1 A Two-Level Rabi System

To understand how a periodic system behaves, we consider a basic quantum mechanical behaviour of a two-level spin $\frac{1}{2}$ system in a periodic magnetic field

Suppose we have a spin $\frac{1}{2}$ system in a static B-field, $\vec{\boldsymbol{B}}_{\boldsymbol{static}}$ along the z-direction plus a rotating magnetic field in the xy-plane, $\vec{\boldsymbol{B}}_{\boldsymbol{rotation}}$ as described pictorially in Figure 1, we want to see how the population of the up and down state evolves with time.

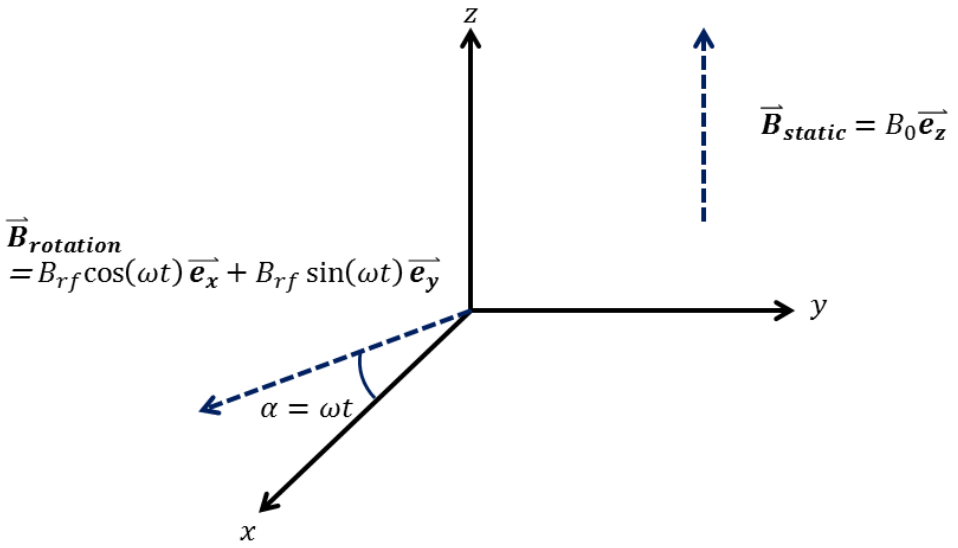

Figure 1 A Spin $\frac{1}{2}$ system in a periodic magnetic field.

From above, the resultant magnetic field is being obtained as follow:

$$\begin{aligned}\overrightarrow{\boldsymbol{B}} &= \overrightarrow{\boldsymbol{B}}_{\boldsymbol{rotational}} + \overrightarrow{\boldsymbol{B}}_{\boldsymbol{static}} \\ &= B_{rf}\, cos(\omega t)\, \vec{\boldsymbol{e}}_{\boldsymbol{x}} + B_{rf}\, sin(\omega t)\, \vec{\boldsymbol{e}}_{y} + B_0 \vec{\boldsymbol{e}}_{\boldsymbol{z}}\end{aligned}$$

where B_{rf} is the magnitude of the applied rotational B-field.

With this expression of the magnetic field, the Hamiltonian, $H(t)$ of the above system with gyromagnetic ratio, γ can also be easily obtained as shown below.

$$\begin{aligned}H(t) &= -\gamma \overrightarrow{\boldsymbol{B}} \cdot \vec{\boldsymbol{S}} \\ &= -\frac{\gamma\hbar}{2} \overrightarrow{\boldsymbol{B}} \cdot \vec{\boldsymbol{\sigma}} \\ &= -\frac{\gamma\hbar}{2} \begin{pmatrix} B_0 & B_{rf}\cos(\omega t) + iB_{rf}\sin(\omega t) \\ B_{rf}\cos(\omega t) - iB_{rf}\sin(\omega t) & -B_0 \end{pmatrix} \\ &= \frac{\gamma\hbar}{2} \begin{pmatrix} B_0 & B_{rf}e^{i\omega t} \\ B_{rf}e^{-i\omega t} & -B_0 \end{pmatrix}\end{aligned}$$

Out of mathematical convenience which will be appreciated later, we let $\gamma B_0 = \omega_0$ and $\gamma B_{rf} = \Omega$ and this reduces the Hamiltonian, $H(t)$ into the following form:

$$H(t) = \begin{pmatrix} -\frac{\hbar\omega_0}{2} & \frac{\hbar\Omega}{2}e^{i\omega t} \\ \frac{\hbar\Omega}{2}e^{-i\omega t} & \frac{\hbar\omega_0}{2} \end{pmatrix}$$

Together with the use of the basis $\left\{\begin{pmatrix}1\\0\end{pmatrix}, \begin{pmatrix}0\\1\end{pmatrix}\right\}$ to represent the spin up and spin down state respectively, a generic state can be expressed clearly as shown below:

$$|\Psi(t)\rangle = c_1(t)\begin{pmatrix}1\\0\end{pmatrix} + c_2(t)\begin{pmatrix}0\\1\end{pmatrix} = \begin{pmatrix}c_1(t)\\c_2(t)\end{pmatrix}$$

Invoking Born's Rule, we understand that the probability of the state of the system being in the spin up state at time t is given by $|c_1(t)|^2$ whereas the state of the system in the spin down state at time t is given by $|c_2(t)|^2$ [27]. Therefore, to study the population evolution of the system it means that we are interested in finding out what are the values of $|c_1(t)|^2$ and $|c_2(t)|^2$ at time, t which can be done via the use of the time-dependent Schrödinger equation. Without further ado, we substitute the Hamiltonian, $H(t)$ and the generic state, $|\Psi(t)\rangle$ into equation (2.3) and the following expression in matrix form can be obtained:

$$i\hbar\frac{\partial}{\partial t}\begin{pmatrix}c_1(t)\\c_2(t)\end{pmatrix}=\begin{pmatrix}-\frac{\hbar\omega_0}{2} & \frac{\hbar\Omega}{2}e^{i\omega t}\\ \frac{\hbar\Omega}{2}e^{-i\omega t} & \frac{\hbar\omega_0}{2}\end{pmatrix}\begin{pmatrix}c_1(t)\\c_2(t)\end{pmatrix}$$

However, due to the Hamiltonian, $H(t)$ being time-dependent, we are unable to make use of equation (2.8) to evolve the state directly. Therefore, if we are able to turn the time-dependent Hamiltonian, $H(t)$ into a time-independent Hamiltonian, it will be much more convenient mathematically for us to tackle the problem. This fortunately can be done via the introduction of a *Dress-State Picture* for the system. A complete explanation of dressing the system can be found in Appendix C of this thesis to help the reader appreciate the usefulness of this mathematical trick.

Upon dressing the system, we get the following form of the time-dependent Schrödinger equation in which the Hamiltonian, $H(t)$ becomes time-independent:

$$i\hbar\frac{\partial}{\partial t}\begin{pmatrix}\widetilde{c_1}(t)\\\widetilde{c_2}(t)\end{pmatrix}=\hbar\begin{pmatrix}\omega-\frac{\omega_0}{2} & \frac{\Omega}{2}\\ \frac{\Omega}{2} & \frac{\omega_0}{2}\end{pmatrix}\begin{pmatrix}\widetilde{c_1}(t)\\\widetilde{c_2}(t)\end{pmatrix}$$

With this time-independent Hamiltonian, we can now make use of equation (2.8) to determine the time-evolution operator, $U(t,t_0)$ easily. Therefore, we had successfully simplified the problem of solving for a time-dependent Hamiltonian by turning it into a problem of solving for the eigenspectrum and eigenstates of the effective time-independent Hamiltonian, H_{eff} which is given by:

$$H_{eff}=\hbar\begin{pmatrix}\omega-\frac{\omega_0}{2} & \frac{\Omega}{2}\\ \frac{\Omega}{2} & \frac{\omega_0}{2}\end{pmatrix}$$

Upon evaluation, the eigenvalues, $E_\pm$ and eigenstates $\{|E_+\rangle, |E_-\rangle\}$ are being obtained as shown below:

$$E_\pm=\frac{\omega\pm\sqrt{(\omega-\omega_0)^2+|\Omega|^2}}{2}\hbar=\frac{(\omega\pm X)\hbar}{2}$$

$$|E_-\rangle=\frac{1}{\sqrt{\Omega^2+Y^2}}\begin{pmatrix}-\Omega\\Y\end{pmatrix}\qquad\text{and}\qquad|E_+\rangle=\frac{1}{\sqrt{\Omega^2+Y^2}}\begin{pmatrix}\mathrm{Y}\\\Omega\end{pmatrix}$$

where $X=\sqrt{(\omega-\omega_0)^2+|\Omega|^2}$ and $Y=X+\omega-\omega_0$ are defined for mathematical convenience as well.

Now, we suppose the initial state of the system is $|\widetilde{\Psi}(0)\rangle = \begin{pmatrix}\widetilde{c_1}(0)\\ \widetilde{c_2}(0)\end{pmatrix} = \begin{pmatrix}1\\0\end{pmatrix}$, then according to equation (2.8), the final state at time, t will be obtained as follow:

$$|\widetilde{\Psi}(t)\rangle = e^{\frac{iE_-}{\hbar}t}\begin{pmatrix}-\Omega\\ Y\end{pmatrix}\left(-\frac{\Omega}{\Omega^2+Y^2}\right) + e^{\frac{iE_+}{\hbar}t}\begin{pmatrix}Y\\ \Omega\end{pmatrix}\left(\frac{\mathrm{Y}}{\Omega^2+Y^2}\right)$$

Therefore, from the above solution it can be easily seen how $\widetilde{c_1}(t)$ and $\widetilde{c_2}(t)$ evolves with time. Furthermore, using Born's Rule, the probability of the system in the spin up and spin down state with respect to time can be calculated and we have the following expressions for them:

$$|\widetilde{c_1}(t)|^2 = 1 - \frac{4Y^2\Omega^2}{(\Omega^2+Y^2)^2}\sin^2\left(\frac{X}{2}t\right) \quad \text{and} \quad |\widetilde{c_2}(t)|^2 = \frac{4Y^2\Omega^2}{(\Omega^2+Y^2)^2}\sin^2\left(\frac{X}{2}t\right)$$

To see how $|\widetilde{c_1}(t)|^2$ and $|\widetilde{c_2}(t)|^2$ evolves with time pictorially, graphs of the population evolution are being plotted against time in Figure 2a-2d with varying driving frequency, ω. From Figure 2a-2d, it is obvious that the system dynamics is stable even when the driving field is detuned because the population evolves coherently and the probabilities do not "blow up" to infinity with respect to time.

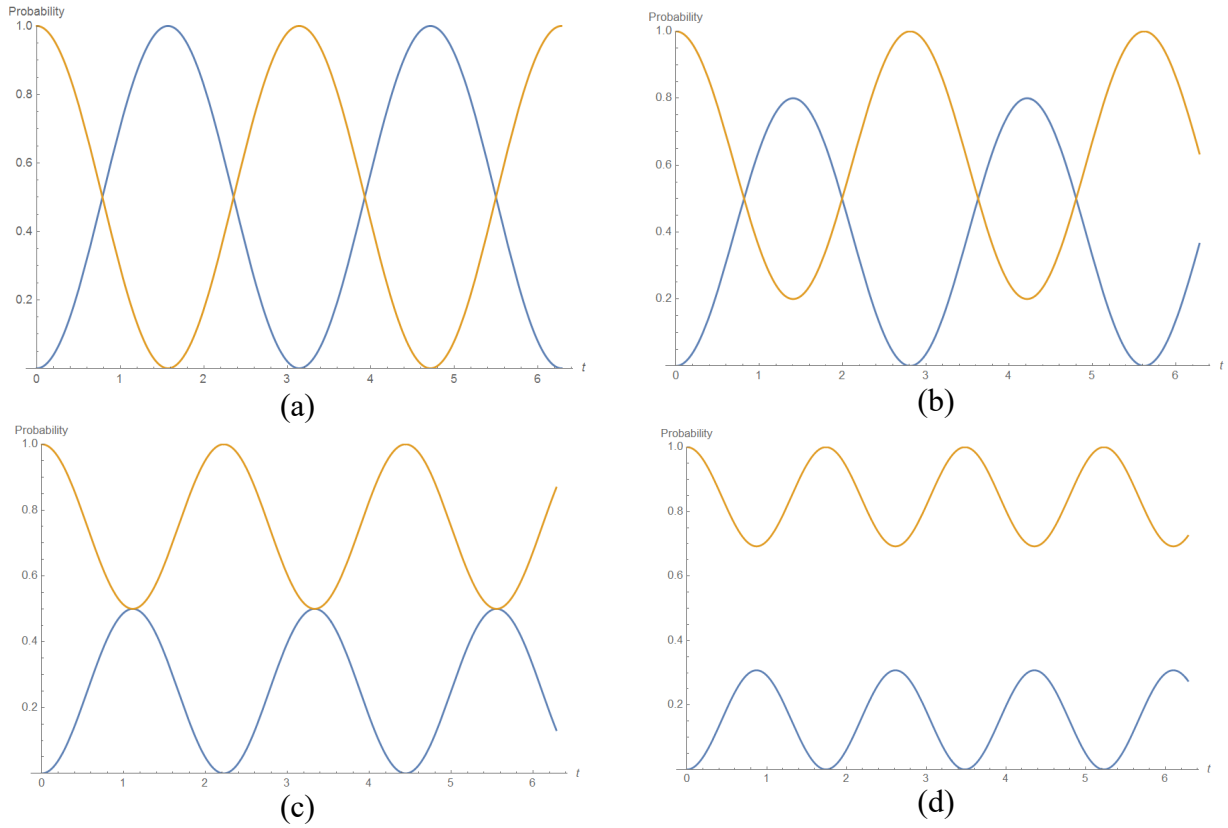

Figure 2 Plots of $|\widetilde{c_1}|^2$ (Orange line) and $|\widetilde{c_2}|^2$(Blue line) against time, t. a) At resonance $\omega = \omega_0$, b) $\omega = 0.95\omega_0$, c) $\omega = 0.90\omega_0$, d) $\omega = 0.85\omega_0$.

Therefore, we came to the conclusion that even though a system is being driven by a periodic field, it does not necessarily mean that the system will evolve in an unstable manner. In fact, periodic driving can be used as a method to stabilize the dynamics of a system. This is a very useful method of stabilizing a system especially for the case whereby non-Hermitian Hamiltonian is being used to describe a dissipating/open system. Additionally, it is also being noted that the above two-level system in a magnetic field can be generalized to a two-level system interacting with laser fields as well. Lastly, other than the dress state picture, smart mathematical techniques such as Rotating Wave Approximation (RWA) or Floquet Formalism can also be deployed at appropriate times to solve this Rabi problem as well [28].

In conclusion, this kind of population evolution of a time-dependent system is also being known as the Rabi oscillation named after Isidor Isaac Rabi who discovered and studied it in 1944. With this, we hoped that the reader can appreciate why a periodic field can be used to stabilize a quantum system and apply this to non-Hermitian systems later.

Chapter 4

Floquet Formalism

4.1 Floquet Theory & Time-Dependent Schrödinger Equation

In view of the need to tackle the problem of periodic Hamiltonians, the Floquet formalism for quantum mechanics can be utilized as a tool for our calculations.

In the study of Ordinary Differential Equations (ODE), the Floquet Theory is being formalized to provide solutions for periodic linear differential equations of the form:

$$\frac{dx}{dt} = A(t)x \tag{4.1}$$

where $A(t)$ is a piecewise continuous periodic function with period, T, i.e. $A(t) = A(t+T)$.

From equation (4.1), we see that it is mathematically similar to our time-dependent Schrödinger equation as shown in equation (2.3). Therefore, when being tasked with the challenge to tackle a time periodic problem in our study of periodically driven non-Hermitian systems, we had found ourselves an advanced and established mathematical tool to handle this problem effectively. Interestingly, in the realm of solid state physics, physicists call this technique the Bloch Wave Theory which is commonly used to determine the band gap energies while mathematicians prefer to call this technique the Floquet Theory [29]. In fact, the Floquet formalism is so useful in tackling periodically time driven Hamiltonians that it had been studied extensively and developed in great depth by Shirley to understand periodic systems in atomic and molecular physics [28]. However, in his paper, the time-dependent Hamiltonian that is being tackled is Hermitian. This condition guarantees a stable system evolution because the closed system has a unitary time evolution operator, $U(t,0)$. On the contrary, in this thesis, the Hamiltonians that are being tackled are non-Hermitian because we are studying open systems with gain and loss. Hence, we will need to be careful not to overgeneralize the theory and use it indiscriminately during our analysis. Despite of this, the Floquet formalism is still very robust and the following section will give a brief introduction to the formalism using Hermitian Hamiltonians. Upon familiarizing ourselves with the basic formalism, the later sections will generalize the theory for usage in tackling non-Hermitian Hamiltonians.

4.2 Floquet Theory

In this section, we shall begin by using a Hermitian, time periodic Hamiltonian (i.e. $H(t) = H^{\dagger}(t)$ and $H(t+T) = H(t)$ where T is the period) to give a basic introduction of the Floquet formalism. Floquet formalism can be utilized to handle such Hamiltonians due to the periodic structure of the Hamiltonian which enables $H(t)$ to obey symmetry under discrete time translation, $t \to t+T$ [47-49]. With this, we can now write our time-dependent Schrödinger equation as follow:

$$\left(H(x,t) - i\hbar\frac{\partial}{\partial t}\right)|\Psi(x,t)\rangle = 0 \tag{4.2}$$

where

$$H(x,t) = H_0(x) + V(x,t) \qquad \text{and} \qquad V(x,t) = V(x,t+T) \tag{4.3}$$

The unperturbed Hamiltonian, $H_0(x)$ is also assumed to possess a complete orthonormal set of eigenstates $\{|\psi_n(x)\rangle\}$ that is associated with eigenvalues $\{E_n\}$. According to the Floquet Theorem, it states that the solution to equation (4.2) has the following form:

$$|\Psi_\alpha(x,t)\rangle = exp\left(-\frac{i\epsilon_\alpha t}{\hbar}\right)|\phi_\alpha(x,t)\rangle \tag{4.4}$$

where $|\phi_\alpha(x,t)\rangle$ is a periodic state known also as a Floquet mode and have the same period, T as the Hamiltonian, $H(t)$ i.e. $|\phi_\alpha(x,t)\rangle = |\phi_\alpha(x,t+T)\rangle$. The ϵ_α in (4.4) are real numbers known as Floquet characteristic components or quasienergies and are unique up to multiples of $\hbar\omega, \omega = \frac{2\pi}{T}$ because the Hamiltonian, $H(t)$ is Hermitian [28,46]. It is also noted that the Floquet theorem can be stated in an alternative form as follow:

$$|\Psi_\alpha(x,t+T)\rangle = \exp\left(-\frac{i\epsilon_\alpha T}{\hbar}\right)|\Psi_\alpha(x,t)\rangle$$

By taking a glance at the Bloch Wave Theory in solid state physics, we can see that the quasienergies are actually analogs of the quasimomentums, $\vec{\boldsymbol{k}}$ that characterize the Bloch eigenstates in a periodic solid and we will study this in chapter 9 of this thesis clearly.

Suppose we perform a substitution of equation (4.4) into equation (4.2), we will obtain an eigenvalue equation for the quasienergy, ϵ_α as follow:

$$H_F(x,t)|\phi_\alpha(x,t)\rangle = \epsilon_\alpha|\phi_\alpha(x,t)\rangle \tag{4.5}$$

where

$$H_F(x,t) = H(x,t) - i\hbar\frac{\partial}{\partial t}$$

From equation (4.5), it is also easily observed that the following Floquet mode in equation (4.6) also produces identical solution to that in equation (4.4) but with a shift in quasienergy shown in equation (4.7).

$$|\phi_{\alpha\prime}(x,t)\rangle = \exp(in\omega t)\,|\phi_\alpha(x,t)\rangle \equiv |\phi_{\alpha n}(x,t)\rangle \tag{4.6}$$

where $n \in \mathbb{Z} = 0, \pm1, \pm2, ...$

$$\epsilon_\alpha \to \epsilon_{\alpha\prime} = \epsilon_\alpha + n\hbar\omega \equiv \epsilon_{\alpha n} \tag{4.7}$$

With this, we can therefore see that the Greek letter α is being used to correspond to a whole class of solutions that are being indexed by $\alpha' = (\alpha, n)$ where $n = 0, \pm1, \pm2, ...$ Since for each quasienergy, ϵ_α there are equivalent quasienergies, $\epsilon_\alpha + n\hbar\omega$, it is possible to reduce an arbitrary quasienergy to a single zone (first Brillouin zone) where $-\frac{\hbar\omega}{2} \le \epsilon < \frac{\hbar\omega}{2}$. Furthermore, it is also convenient for us to introduce a composite Hilbert space $\mathcal{R} \otimes \mathcal{T}$ for the Floquet Hamiltonian, $H_F(x,t)$ where $\mathcal{R}$ is the Hilbert space of the square integrable functions on the configuration space and $\mathcal{T}$ as the space of functions which are periodic in t with period, $T = \frac{2\pi}{\omega}$ [50]. This therefore gives us the definition of the inner product of the spatial parts as:

$$\langle\psi_n(x)|\psi_m(x)\rangle = \int_{-\infty}^{\infty} \psi_n^*(x)\psi_m(x)dx = \delta_{n,m} \tag{4.8}$$

For the time components, because it is being spanned by the orthonormal set of Fourier vectors defined as follow: $\langle t|n\rangle = \exp(in\omega t)$, the inner product in the $\mathcal{T}$ space is defined as:

$$(m,n) = \frac{1}{T}\int_0^T \exp[i(n-m)\omega t]\,dt = \delta_{n,m} \tag{4.9}$$

Combining the definitions of inner product in both $\mathcal{R}$ and $\mathcal{T}$ space, we can conclude that the Floquet modes of $H_F(x,t)$ obeys orthonormality condition in the composite Hilbert space $\mathcal{R} \otimes \mathcal{T}$. With this, Sambe [50] gave the following definition for the Floquet modes:

$$\left\langle\left\langle\phi_{\alpha'}(x,t)\middle|\phi_{\beta'}(x,t)\right\rangle\right\rangle = \frac{1}{T}\int_0^T dt \int_{-\infty}^{\infty} dx\ \phi_{\alpha'}^*(x,t)\phi_{\beta'}(x,t) \tag{4.10}$$

$$= \frac{1}{T}\int_0^T dt \exp[i(m-n)\omega t] \int_{-\infty}^{\infty} dx\, \phi_\alpha^*(x,t)\phi_\beta(x,t)$$

$$= \left\langle \left\langle \phi_{\alpha n}(x,t) \middle| \phi_{\beta m}(x,t) \right\rangle \right\rangle$$

$$= \delta_{\alpha,\beta}\delta_{n,m}$$

In additionally, the Floquet modes also form a complete set in $\mathcal{R} \otimes \mathcal{T}$ as follow:

$$\sum_{\alpha,n} \phi_{\alpha n}^*(x,t)\phi_{\alpha n}(x',t') = \delta(x-x')\delta(t-t') \tag{4.11}$$

With the groundwork being set clear, we shall now go on to section 4.3 where we understand how the time evolution operator behaves for Floquet Hamiltonians.

4.3 Time Evolution Operator for Floquet Hamiltonians

To understand how the system under such periodic Hamiltonians evolves, we can make use of the time evolution operator, $U(t,t_0)$ to evolve the state of the system with respect to time. Given the definition of a time evolution operator, $U(t,t_0)$ by equation (2.4) and equation (2.5), it can be shown that $U(t,t_0)$ have special mathematical properties when $H(t)$ is periodic. To illustrate as an example, we realize that $U(t,t_0)$ over a complete period, T can be used to evolve an initial state over long multiples of the fundamental period shown as follow:

$$U(NT,0) = U^N(T,0) \tag{4.12}$$

To see why equation (4.12) is true, a short proof is given below:

Proof

Invoking equation (2.7) and setting $t_0 = 0$, the following expression is being obtained due to the periodicity of $H(t)$:

$$U(NT,0) = \boldsymbol{T}exp\left[-\frac{i}{\hbar}\int_0^{NT} H(t')dt'\right]$$

$$= \boldsymbol{T}exp\left[-\frac{i}{\hbar}\sum_{k=1}^{N}\int_{(k-1)T}^{kT} H(t')dt'\right]$$

where $\boldsymbol{T}$ is the time-ordering operator.

Since $H(t') = H(t'+T)$, we can further simplify the expression into:

$$U(NT,0) = \boldsymbol{T}exp\left[-\frac{i}{\hbar}\sum_{k=1}^{N}\int_0^T H(t')dt'\right]$$

$$= \boldsymbol{T}\prod_{k=1}^{N} exp\left[-\frac{i}{\hbar}\int_0^T H(t')dt'\right] \tag{4.13}$$

Since the terms over a complete period are equal, they commute with one another. As a result, we can now shift the time-ordering operator to the front of a single term and obtain equation (4.14) as follow:

$$U(NT,0) = \prod_{k=1}^{N}\boldsymbol{T}exp\left[-\frac{i}{\hbar}\int_0^T H(t')dt'\right]$$

$$= U^N(T,0) \tag{4.14}$$

(QED)

With this, one can also show that when $t_0 = 0$, equation (4.15) and equation (4.16) hold as follow:

$$U(t+T,T) = U(t,0) \tag{4.15}$$

and this implies that

$$U(t+T,0) = U(t,0)U(T,0) \tag{4.16}$$

It is important to note that in equation (4.16), $U(t,0)$ does not commute with $U(T,0)$ except when $t = NT$. Furthermore, it is essential for us to appreciate the usefulness of equation (4.12) because once we have the knowledge of $U(T,0)$ over a fundamental period, $T = \frac{2\pi}{\omega}$, it will give us all the necessary information required to study the long run dynamics of a periodically driven system.

To see how the state of a system evolves dynamically in time, we suppose the initial state of the system is given by equation (4.17) and is expanded in the Floquet modes' basis.

$$|\Psi(x,t_0)\rangle = \sum_{\alpha} c_\alpha |\phi_\alpha(x,t_0)\rangle \tag{4.17}$$

Substituting equation (4.17) into equation (2.4), we get the expression of the final state as:

$$|\Psi(x,t+t_0)\rangle = U(t+t_0,t_0)\sum_{\alpha} c_\alpha |\phi_\alpha(x,t_0)\rangle$$

$$= \sum_{\alpha} c_{\alpha} \exp\left(-\frac{i\epsilon_{\alpha} t}{\hbar}\right) |\phi_{\alpha}(x, t_0)\rangle \tag{4.18}$$

In particular, when $t_0 = 0$, $t = NT$, we see that,

$$\begin{aligned} |\Psi(x, NT)\rangle &= U(NT, 0) \sum_{\alpha} c_{\alpha} |\phi_{\alpha}(x, 0)\rangle \\ &= U^N(T, 0) \sum_{\alpha} c_{\alpha} |\phi_{\alpha}(x, 0)\rangle \\ &= \sum_{\alpha} c_{\alpha} \exp\left(-N\frac{i\epsilon_{\alpha} T}{\hbar}\right) |\phi_{\alpha}(x, 0)\rangle \end{aligned} \tag{4.19}$$

Equation (4.18) and equation (4.19) can be simplified as above into terms involving quasienergies instead of the Hamiltonians because in linear algebra, it is being stated that a matrix exponential, e^H shares the same set of eigenstates with the matrix H itself and has eigenvalues of the form of $e^{\epsilon_{\alpha}}$ [38]. Thus, we see that the Floquet modes are actually Floquet eigenstates for the time evolution operator (Floquet operator) and hence arrive at equation (4.20) which will be use in later chapters extensively.

$$U(T, 0)|\phi_{\alpha}(x, t)\rangle = \exp\left(-\frac{i\epsilon_{\alpha} T}{\hbar}\right) |\phi_{\alpha}(x, t)\rangle \tag{4.20}$$

In conclusion, we hope that the above presentation gives a basic introduction for the reader to grasp the idea of Floquet Formalism and generalize it to handle non-Hermitian systems that will be described in section 4.4.

4.4 Floquet Theory in Non-Hermitian Systems

In section 4.2 and 4.3, we discussed for the case of a Hermitian periodically driven Hamiltonian. However, for this thesis, since we are handling non-Hermitian periodic Hamiltonians, there will be a few points that we need to take note when applying Floquet theory for calculation.

First of all, when the Hamiltonian is non-Hermitian, the time evolution operator, $U(t, t_0)$ is in general not a unitary operator. As a result, equation (2.9) no longer hold true and probability conservation of the system is no longer obeyed (from a closed system to an open system). This also results in the emergence of imaginary values for the quasienergies, ϵ_{α} and the eigenvalues of the Floquet operator is no longer just a phase factor anymore. Since the eigenvalues of the Floquet operator are now exponential factors, an operation of the Floquet operator on the Floquet

eigenstates will result in an exponential growth of the eigenstates. Given that the state of the system can be expressed in the Floquet eigenstate basis, we will see in chapter 5 that this phenomenon will result in an unstable system dynamics.

However, despite of these, it had been discovered that at certain system parameters and periodic driving of a non-Hermitian Hamiltonian, the time evolution operator for one complete period evolution (Floquet operator), $U(T,0)$ is still unitary because the quasienergies, ϵ_α are real numbers at the start and end of the period. This therefore makes the study of such phenomena an interesting one and we will study about them numerically in chapter 6 and ask: under what conditions this occurs?

In essence, Floquet formalism is a well-established mathematical tool that offers us a way to tackle the time-dependent Schrödinger equation involving periodic Hamiltonians. With these understandings, we can now apply it to tackle periodic, non-Hermitian Hamiltonians and check for stability of such systems under periodic driving.

Chapter 5

Extended Unitarity & Restoring Stability

In view of the need to describe dissipative/open system using non-Hermitian Hamiltonians, we are going to study about them deeper in this thesis and understand clearly why stabilization of such a system is possible by periodic driving. In this chapter, we will put forward definition for some terminologies that will be used in later chapters for the reader to have a better understanding of their meaning when the terms are being used.

5.1 Defining Extended Unitarity

With regards to the proof of unitarity of the time evolution operator, $U(t, t_0)$ in chapter 1, we see the importance of the Hermiticity condition of the Hamiltonian, $H(t)$. With this condition being fulfilled, it guarantees the unitarity of the time evolution operator, $U(t, t_0)$. This therefore inspired us to ask the following question: *What will happen if the Hamiltonian is no longer Hermitian?* Taking a look at equation (2.6), we see that a unitary time evolution operator, $U(t, t_0)$ fits nicely into the equation when the Hamiltonian is Hermitian. However, when a time-dependent, non-Hermitian Hamiltonian is being encountered, the time evolution operator $U(t, t_0)$ is in general non-unitary [37]. As a result, associated with this is an exponentially growth inducing or decay inducing $U(t, t_0)$ which will make the open quantum mechanical system of study an unstable one.

However, upon studying such systems deeper, we discovered that by applying a periodic driving function with period, T to a time-dependent, non-Hermitian Hamiltonian prepared at certain system parameters, we are still able to obtain a unitary time-evolution operator, $U(t, t_0)$ for the system at certain times. However, this time evolution operator will only be unitary and satisfy equation (2.6) at times which are equal to integer multiples of the period, T. *With this, we state that a time evolution operator or specifically the Floquet operator, $U(T + t_0, t_0)$ of a time-dependent, non-Hermitian Hamiltonian possesses Extended Unitarity when it only introduces a phase factor to the Floquet eigenstate of the system upon N arbitrary number of driving periods, T, where N is an integer. (Note: The evolution operator does not need to obey extended unitarity*

condition at all time, t' where $t < t' < t + T$. It only needs to satisfy the condition at the start and end of a period or multiples times of the period shown later in Chapter 6)

5.2 Restoring Stability via Periodic Driving

After familiarizing ourselves with the Floquet Formalism, dynamics of a two-level periodically driven system and understanding the rationale behind non-Hermitian Hamiltonians, we are now ready to tackle the issue at hand.

To reduce overgeneralization for the scope of this thesis, the periodic functions that we used to drive the system in this thesis are smooth, well defined functions and do not contain any point of singularity. Hence periodic functions such as $\tan(t)$, $\sec(t)$ and $cosec(t)$ that possess point of singularity will not be discussed here.

Now, suppose we are given a time-dependent, non-Hermitian Hamiltonian, we can attempt to stabilize the system via the use of periodic driving. While the system is being periodically driven, we can check the time-evolution operator, $U(t, t_0)$ for extended unitarity at times after *N* integer multiples of the period, T. If the time evolution operator fulfills extended unitarity condition, we will conclude that the system is being stabilized. This is because the Floquet eigenstates actually form a complete basis set and thus any initial state of the system, $|\Psi(t_0)\rangle$ can be expressed as a linear combination of the Floquet eigenstates. If the time evolution operator fulfills extended unitarity condition, it will only introduce a phase factor to the Floquet eigenstates after some *NT* time evolution without blowing up or decaying any of the eigenstates at all. This therefore ensures that $|\Psi(t_0)\rangle$ which is now expressed as a linear combination of the Floquet eigenstates does not blow up or decay as well after some *NT* time evolutions, thereby stabilizing the system.

To comprehend the above qualitative description quantitatively, we can make use of Floquet formalism that was being introduced in Chapter 3 to aid our understanding. According to Floquet theory, to prevent confusion, the time evolution operator associated with $H(t)$ after a period, T is given a special name known as the Floquet operator, $U(T + t_0, t_0)$. Furthermore, it will have eigenspectrum that can be represented via the following equation:

$$U(T + t_0, t_0)|\phi_n\rangle = e^{i\beta_n}|\phi_n\rangle$$

where $|\phi_n\rangle$ is the nth Floquet eigenstate and $e^{i\beta_n}$ is the eigenvalues of the Floquet operator. From the above, we see that when all the eigenphases, $\beta_n = -\frac{\epsilon_\alpha T}{\hbar}$ are just real numbers, then, all the eigenvalues of the Floquet operator will just be purely phase factors. This will thereby ensures that the Floquet operator is a unitary operator up to a similarity transformation and hence satisfies extended unitarity condition. In addition, it is also being noted that the Floquet eigenstates form a complete set of basis as follow:

$$I = \sum_n |\phi_n\rangle\langle\phi_n|$$

Upon fulfilling the above extended unitarity condition, we can write the Floquet operator after 1 period evolution in the following form:

$$U(T + t_0, t_0) = SDS^{-1}$$

where D is a unitary diagonal matrix with the diagonal consisting of $e^{i\beta_n}$ and S as a similarity transformation. This diagonalization of the Floquet operator is of great mathematical convenience especially when we are required to compute recurring matrix multiplication. With this, we can easily see that after N period time evolution, the Floquet operator will become:

$$U(NT + t_0, t_0) = SD^N S^{-1}$$

and similarly, the Floquet eigenstates will only acquire a pure phase factor of $e^{iN\beta_n}$ after arbitrary N driving periods.

Now, if we apply the Floquet operator, $U(NT + t_0, t_0)$ which fulfills extended unitarity condition to an initial state of the system, $|\Psi(t_0)\rangle$ we can easily see that the system's dynamics is stable without any exponential growth or decay as shown below:

$$\begin{aligned} U(NT + t_0, t_0)|\Psi(t_0)\rangle &= U(NT + t_0, t_0) \sum_n c_n |\phi_n\rangle \\ &= U^N(T + t_0, t_0) \sum_n c_n |\phi_n\rangle \\ &= \sum_n c_n e^{iN\beta_n} |\phi_n\rangle \end{aligned}$$

In conclusion, we are able to understand the meaning of extended unitarity and see quantitatively why periodic driving is able to stabilize the dynamics of an open system that is being described by a time-dependent, non-Hermitian Hamiltonian. The next chapter will go on to

demonstrate using numerical computation of such systems to give a clearer picture of what is being discussed in this chapter.

Chapter 6

Computational Examples

In the following chapter, the Hamiltonians that are being used to illustrate the idea of extended unitarity are periodic in time $H(t) = H(t+T)$ with T being the driving period. Furthermore, we also scale the Hamiltonians that are used such that they have dimensionless units and $\hbar = 1$.

6.1 A Simple Two-Level System

To begin with, we perform an in depth study on the following time-dependent, non-Hermitian Hamiltonian of a simple two level system that is being driven by a periodic sinusoidal function.

$$H_1(t) = \gamma\,\sigma_z + i\mu\,\sin(t)\,\sigma_x = \begin{pmatrix} \gamma & i\mu\sin(t) \\ i\mu\sin(t) & -\gamma \end{pmatrix}$$

This is a very good and simple example whereby a time periodic, non-Hermitian term $i\mu sin(t)$ is being introduced to a two-level Rabi model parametrized by 2 real parameters γ and μ. With this, a numerical analysis of $H_1(t)$ using Mathematica is being performed at period $T = 2\pi$ to determine the domains of γ and μ whereby extended unitarity condition is being fulfilled. To do so, we scan through numerical values of γ and μ carefully and checked the Floquet spectrum for unity i.e. |eigenvalues of $U(2\pi, 0)| = 1$. Numerical values of γ and μ that satisfy this will be recorded and plotted on a phase diagram as indicated by the shaded domains in Figure 3. The shaded domains therefore mark the region whereby extended unitarity condition is being fulfilled and stabilization of the non-Hermitian system, $H_1(t)$ is possible by periodic driving. Hence, we have shown numerically that contrary to naïve thinking, extended unitarity do not happen accidentally. Instead, there is a wide, continuous and well defined range of γ and μ that fulfill the condition. More details on the exact computational code used can be found in Appendix A.

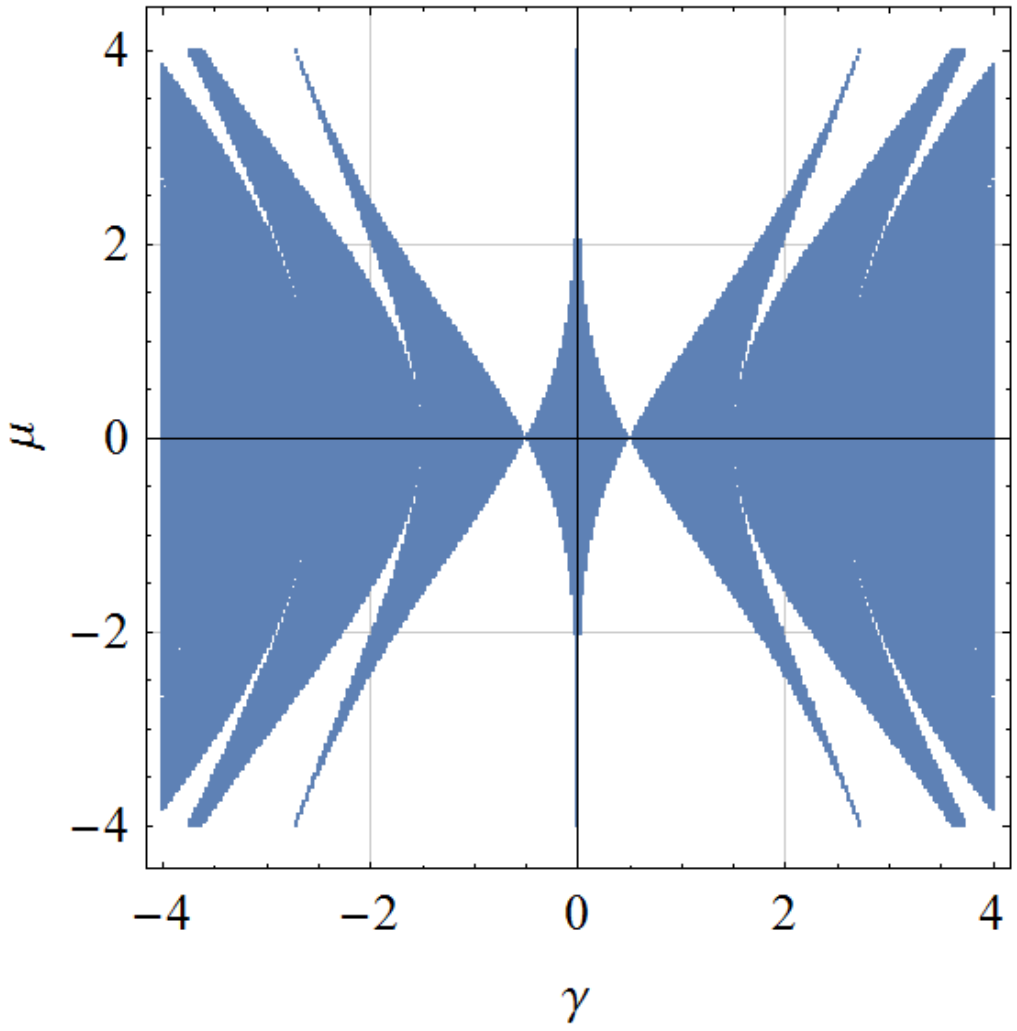

Figure 3 Phase Diagram for parameters $(\boldsymbol{\gamma}, \boldsymbol{\mu})$ for Hamiltonian, $\boldsymbol{H_1(t)}$. Shaded regions are domains of $\boldsymbol{\gamma}, \boldsymbol{\mu}$ whereby extended unitarity condition is fulfilled.

Upon further evaluation, it is also being noted that $H_1(t)$ has the following eigenvalues: $E_{\pm}(t) = \pm\sqrt{\gamma^2 - \frac{\mu^2}{2}[1 - \cos(2t)]}$ at any time, t. By observing the expression of the eigenvalues, we understand without much difficulties that $E_{\pm}$ can be complex for some values of γ and μ at certain times, t within a period $0 \leq t \leq 2\pi$. However, this does not compromise whether γ and μ are successful in fulfilling extended unitarity conditions or not. Taking for example, $\gamma = 2$ and $\mu = 2.25$ (which fulfill extended unitarity condition), we plot the eigenvalues, E_- and E_+ against time for $H_1(t)$ in Figure 4a and 4b. In both figures, we see that there are times within a period whereby the eigenvalues E_- and E_+ are complex but extended

unitarity condition is still nonetheless being fulfilled for these set of parameters($\gamma = 2, \mu = 2.25$).

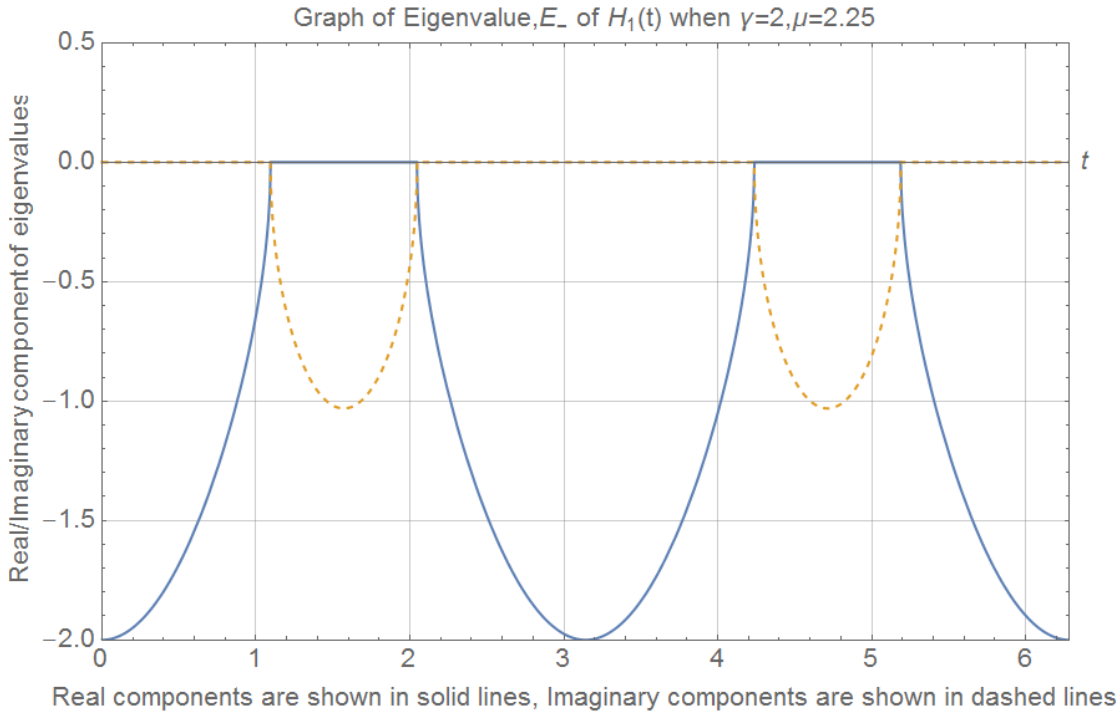

Figure 4a Time evolution of the real and imaginary component of Eigenvalue, $\boldsymbol{E_-}$ for Hamiltonian $\boldsymbol{H_1(t)}$ when $\boldsymbol{\gamma = 2, \mu = 2.25}$ in one period.

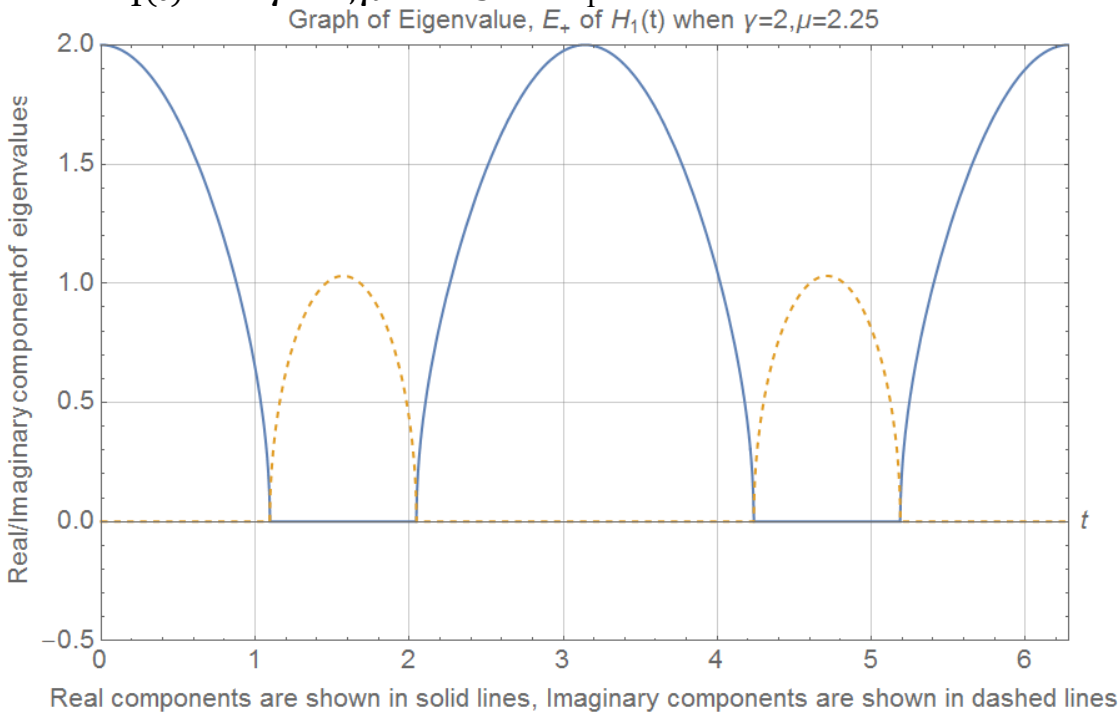

Figure 4b Time evolution of the real and imaginary component of Eigenvalue, $\boldsymbol{E_+}$ for Hamiltonian $\boldsymbol{H_1(t)}$ when $\boldsymbol{\gamma = 2, \mu = 2.25}$ in one period.

Hence, we arrived at the important emphasis and conclusion that: *Extended unitarity condition can still be fulfilled without the need for the time-dependent non-Hermitian Hamiltonian to have completely real instantaneous eigenspectrum at all times.*

After studying the energy eigenspectrum of the Hamiltonian, $H_1(t)$, we can also take a look at the eigenvalues of the evolution operator, $U(t,0)$ at different time, t within a period ($0 \leq t \leq 2\pi$) and observe how it eventually evolves into the Floquet operator when $t = 2\pi$. However, before we go on to study this, it would be useful for us to note that the Hamiltonian, $H_1(t)$ that we are studying is traceless. This is because, according to Liouville's formula, for a two-level Hamiltonian which is traceless, we can write the eigenvalues of the evolution operator, $U(t,0)$ in the form of $e^{\pm i\beta}$ with β being a real number. This will thus show that the real components of the 2 eigenvalues of $U(t,0)$ are identical. A short verification of this can be found in Appendix B.

Equipped with this knowledge, we can proceed to study the system more efficiently now by observing how the real component of the 2 eigenvalues evolve with time within a period at different domains of (γ, μ). To facilitate understanding of the meaning of extended unitarity, we are going to scan from a region whereby the domains (γ, μ) do not satisfy extended unitarity to a region whereby extended unitarity condition is being fulfilled. As an example, by fixing $\gamma = 2$ and varying μ from 1.75 to 2.05 at 0.1 increments we can plot the real components of the 2 eigenvalues of $U(t,0)$ against time as shown in Figure 5a to 5d. This will thus help us observe pictorially how the real component of the 2 eigenvalues evolve with time within a period and account for this behaviour using the concept of extended unitarity.

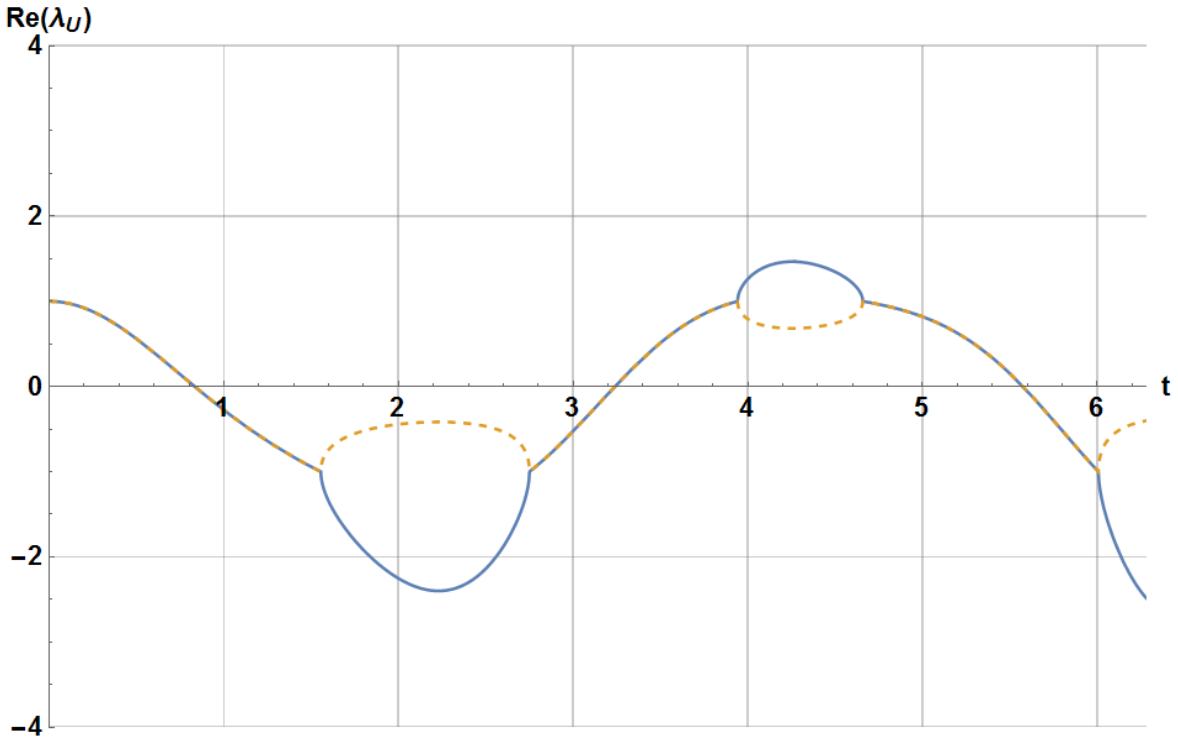

Figure 5a Plots of the real components of the 2 eigenvalues of $U(t,0)$ against time, t when $\gamma = 2, \mu = 1.75$.

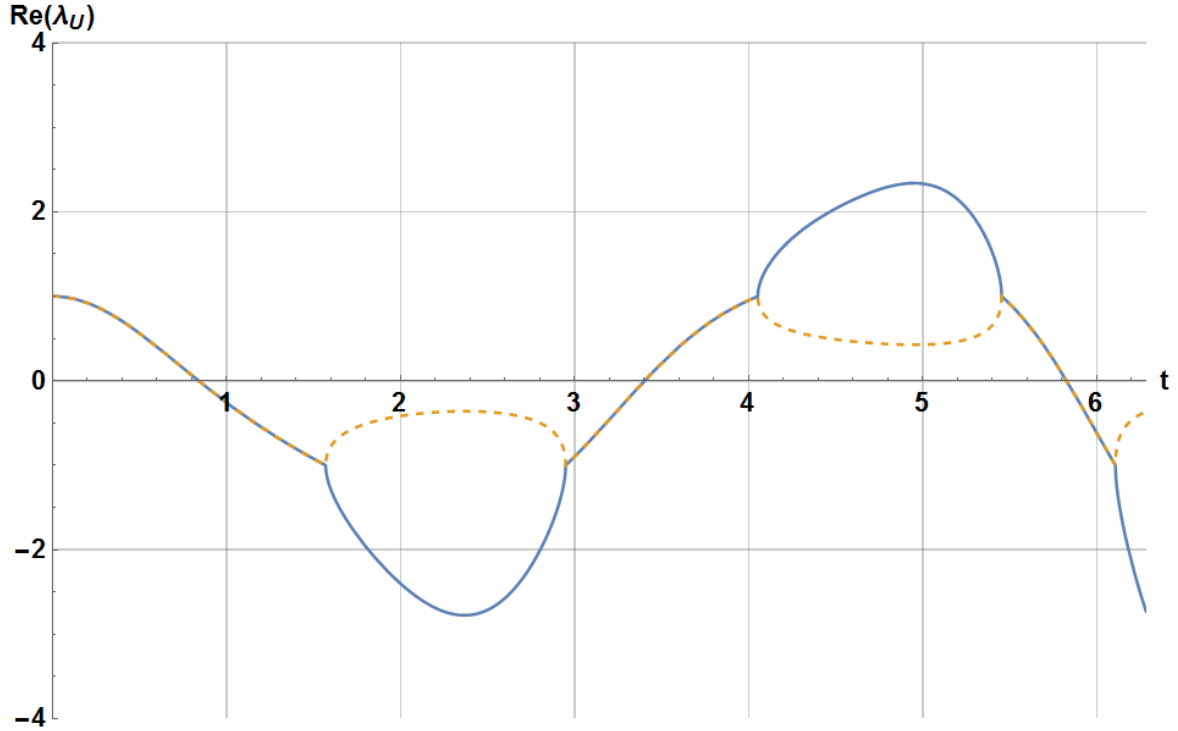

Figure 5b Plots of the real components of the 2 eigenvalues of $U(t,0)$ against time, t when $\gamma = 2, \mu = 1.85$.

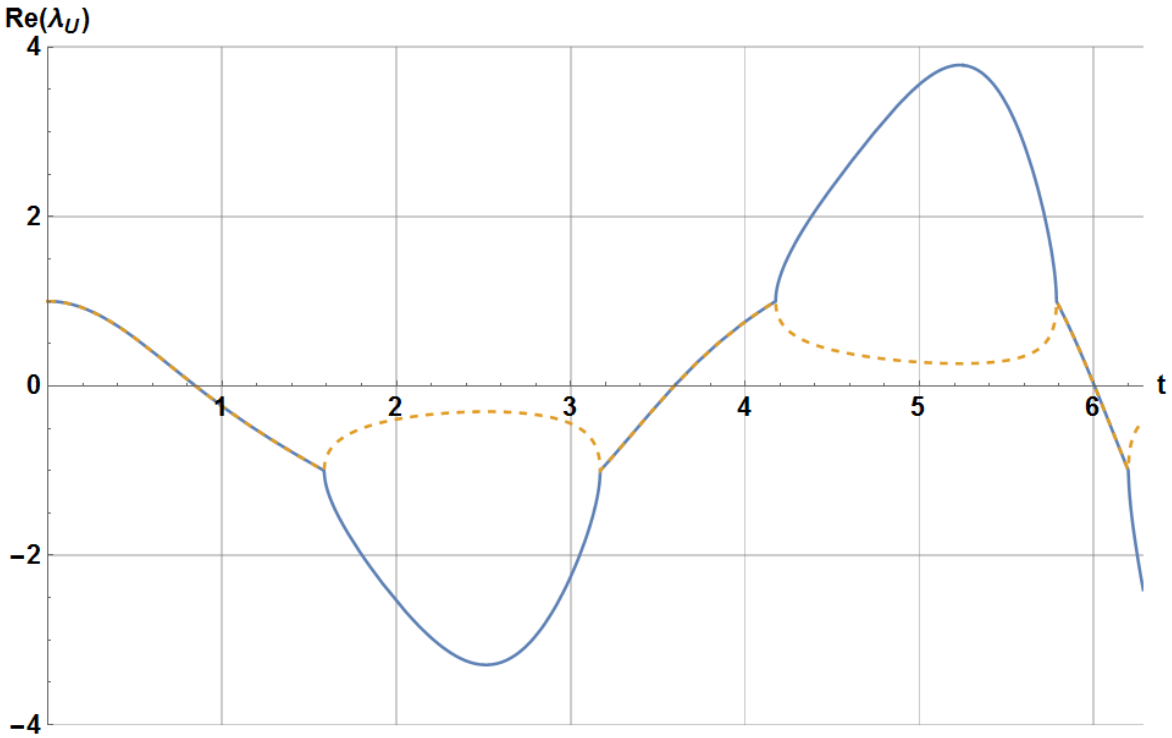

Figure 5c Plots of the real components of the 2 eigenvalues of $\boldsymbol{U(t,0)}$ against time, t when $\boldsymbol{\gamma = 2, \mu = 1.95}$.

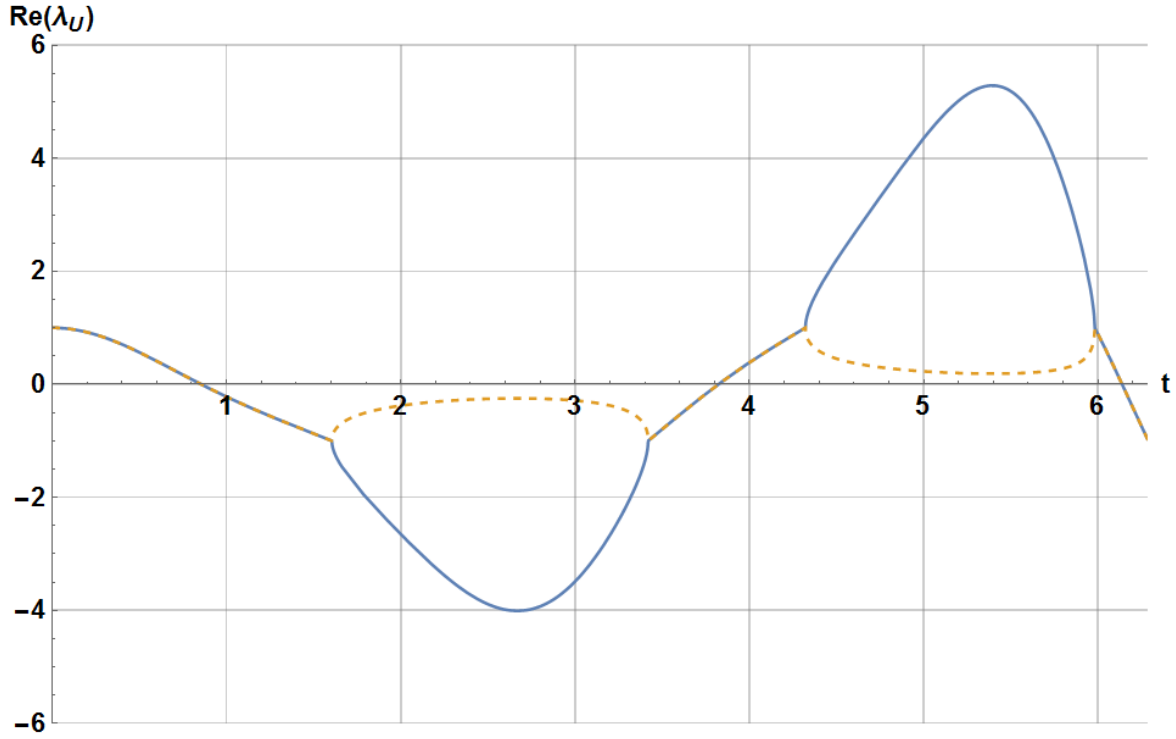

Figure 5d Plots of the real components of the 2 eigenvalues of $\boldsymbol{U(t,0)}$ against time, t when $\boldsymbol{\gamma = 2, \mu = 2.05}$.

In all the plots shown in Figure 5, we observed that the real components of the 2 eigenvalues of $U(t,0)$ spilt from a common value and recombine at some later time, t. Furthermore, this phenomenon of splitting and recombination is also seen to occur many times within a period regardless of whether extended unitarity condition is fulfilled or not. However, the most important and distinct feature that occurs when extended unitarity is satisfied is depicted in Figure 5d whereby the real component of the eigenvalues recombine at the end of 1 period at $T = 2\pi$.

With this, we arrive at another result: *In the domain of extended unitarity, the evolution operator* $U(t,0)$ *does not necessarily need to have real eigenphases,* β *at all time,* t*. As long as the eigenphases are real at multiple periods of* T*, we say that extended unitarity condition is being fulfilled.* Hence, we see that in cases where extended unitarity condition is being satisfied, there is still some interesting and fascinating dynamics that happens within the period.

6.2 Introduction of a Third Parameter ϵ

In this section, a third parameter, ϵ will be introduced to the 2 level Hamiltonian, $H_1(t)$ such that there is a component now that is parallel to the non-Hermitian driving term. As a result, we arrived at a new Hamiltonian, $H_2(t)$ which we will study in this section.

$$H_2(t) = \gamma\,\sigma_z + (\epsilon + i\mu\sin(t))\sigma_x = \begin{pmatrix} \gamma & \epsilon + i\mu\sin(t) \\ \epsilon + i\mu\sin(t) & -\gamma \end{pmatrix}$$

With $H_2(t)$ in hand, a scan for extended unitarity can be done by varying ϵ from $0 \leq \epsilon \leq 3.5$ in 0.5 increments and similar phase diagrams as shown in section 6.1 are being plotted for different values of ϵ in Figure 6.

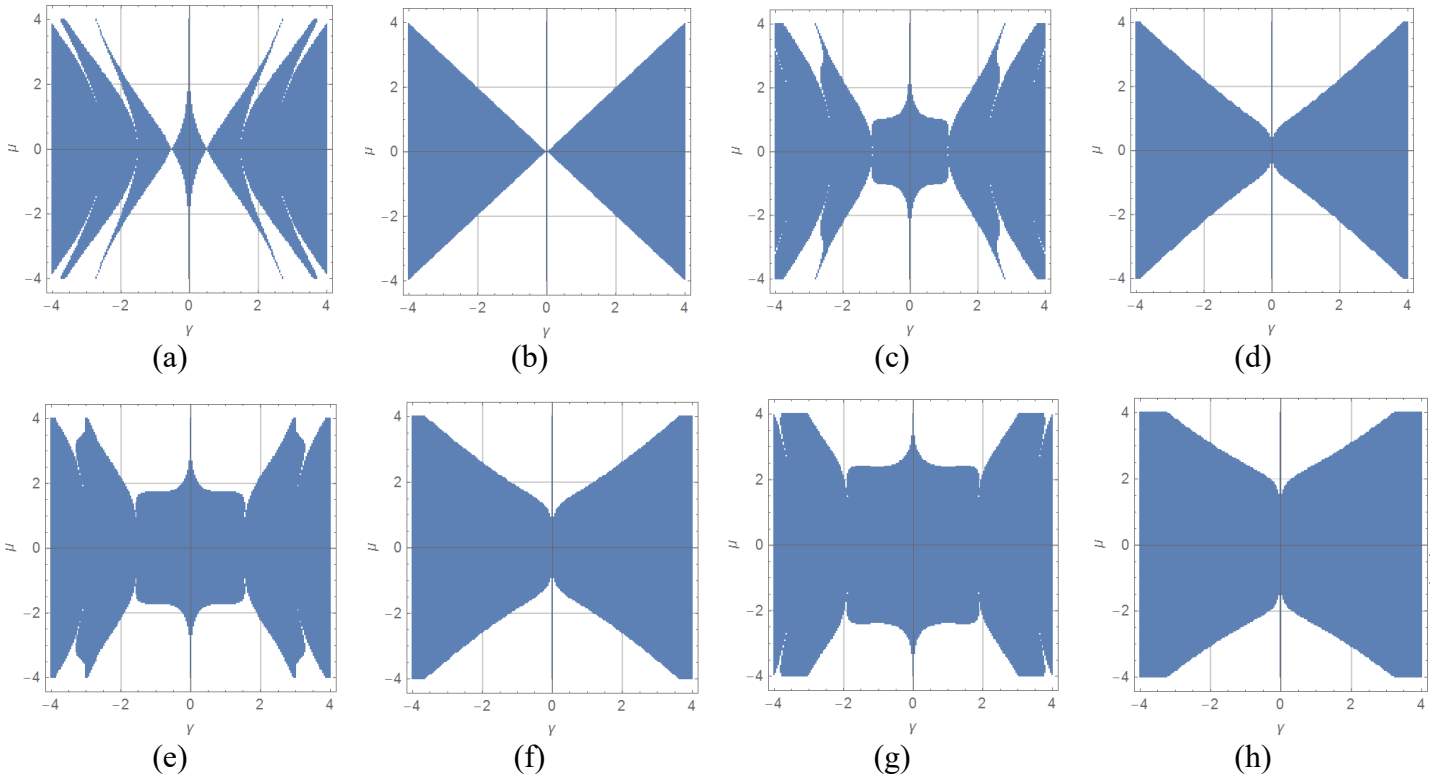

Figure 6 Phase diagram for parameters $\boldsymbol{\gamma, \mu}$ for Hamiltonian, $\boldsymbol{H_2(t)}$ with varying $\boldsymbol{\epsilon}$ (a) $\boldsymbol{\epsilon = 0}$, (b) $\boldsymbol{\epsilon = 0.5}$, (c) $\boldsymbol{\epsilon = 1.0}$, (d) $\boldsymbol{\epsilon = 1.5}$, (e) $\boldsymbol{\epsilon = 2.0}$, (f) $\boldsymbol{\epsilon = 2.5}$, (g) $\boldsymbol{\epsilon = 3.0}$ and (h) $\boldsymbol{\epsilon = 3.5}$. Shaded regions are domains of $\boldsymbol{\gamma, \mu}$ whereby extended unitarity condition is fulfilled.

Therefore, we see that the introduction of a third variable still allows the non-Hermitian system to be stabilized via periodic driving because there are still domains whereby extended unitarity condition is being fulfilled. Furthermore, in this particular case, we can see that as ϵ increases in magnitude, the domains whereby extended unitarity condition is being fulfilled actually increases. This is because when the strength of ϵ increases, it contributes more and more significantly to the interaction between the 2 states as compared to the non-Hermitian periodic driving term. A 3-dimensional phases diagram is not shown here due to the difficulties of presenting a high dimensional phase diagram on a paper itself. Similar analysis on the evolution operator and eigenvalues of $H_2(t)$ can be performed as in section 6.1 and it will yield us similar result in domains where extended unitarity is fulfilled too.

In conclusion, this section illustrates *that extended unitarity conditions and hence stabilization of a non-Hermitian quantum system is still possible even after a third parameter, ϵ is being introduced.* The result that is being affected after introduction of more system

parameters is that the range of the domains of (γ, μ) might vary depending on the strength and direction of the system parameter being introduced.

6.3 More General Periodic Driving Fields

After studying the case whereby more parameters are being introduced to the basic Hamiltonian, $H_1(t)$ we shall now go on to more general cases of Hamiltonians. Taking a look at the following Hamiltonian, $H_3(t)$ with a general periodic driving field that compose of a sine and cosine term with different frequencies, we see that the periodic driving field is not purely sinusoidal. In this section, we are going to demonstrate that in fact, any periodic function that can be decomposed into Fourier series can be used to drive the system and stabilize it [5] as long as it does not possess any singularity point within the period.

$$H_3(t) = \gamma\,\sigma_z + i\mu[\cos(t) + \sin(2t)]\sigma_x = \begin{pmatrix} \gamma & i\mu[\cos(t) + \sin(2t)] \\ i\mu[\cos(t) + \sin(2t)] & -\gamma \end{pmatrix}$$

By performing similar evaluation as in sections 6.1 and 6.2, we get the following phase diagram in Figure 7. As shown in the figure we still see a well-defined and continuous domain of (γ, μ) whereby extended unitarity are being fulfilled even when the periodic driving function is not a simple sine function.

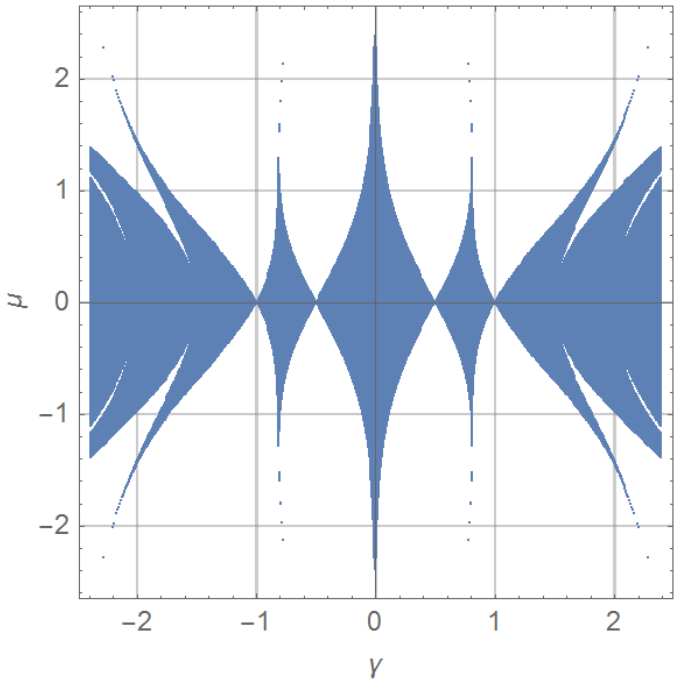

Figure 7 Phase Diagram for parameters $\boldsymbol{\gamma, \mu}$ for Hamiltonian, $\boldsymbol{H_3(t)}$. Shaded regions are domains of $\boldsymbol{\gamma, \mu}$ whereby extended unitarity condition is fulfilled.

Therefore, in this section, we come to the conclusion that *any periodic driving field that is well behaved (do not possess singularities) and can be decomposed into Fourier series (It needs not be purely sinusoidal) can be used to drive the non-Hermitian quantum system and stabilize it by fulfilling extended unitarity conditions in the continuous and well-defined domain of* (γ, μ).

Wrapping up this chapter, we can appreciate the usefulness of Mathematica in helping us numerically analyze these non-Hermitian quantum systems which will be tedious if one were to try and study them analytically. Furthermore, from these numerical analyses, we also come out with four important conclusions about these non-Hermitian periodically driven systems. With this, we shall go on to the next chapter whereby a more general type of Rabi oscillation which we termed it as "Generalized Rabi oscillation" is being utilized to help the reader understand how a non-Hermitian system can be stabilized by periodic driving.

Chapter 7

Generalized Rabi Oscillation

Since we are studying time-dependent quantum systems, and equipped with the knowledge of Rabi oscillations illustrated in Chapter 2, we are motivated to generalize this idea to study the dynamics of non-Hermitian, time-dependent systems. In this chapter, by performing a population evaluation, we discovered the existence of a coherent but non-norm-preserving oscillation which we name it as "Generalized Rabi oscillations". In addition, we shall now highlight the importance of the concept of extended unitarity and the role it plays in stabilizing a non-Hermitian system in this chapter.

7.1 Dynamical study of Hamiltonian, $\boldsymbol{H_1(t)}$

To further understand the dynamics of the system, we study the domains of (γ, μ) whereby extended unitarity conditions are being fulfilled and compare it with domains whereby it is not. Taking a look at the point $(\gamma = 2, \mu = 2.05)$ and $(\gamma = 2, \mu = 1.95)$ as studied in section 6.1, we note that the latter point does not fulfill extended unitarity condition while the former does. By performing a population calculation from an initial "up-state", we see from Figure 8a and 8b that for the case of $(\gamma = 2, \mu = 1.95)$, the population for both states blow up quickly after a few period of driving. This therefore shows that at domains whereby extended unitarity is not being fulfilled, the system will evolve in an unstable manner with their population experiencing an exponential growth quickly with time. Thus, periodic driving at these particular system parameters will not be successful in stabilizing the non-Hermitian system.

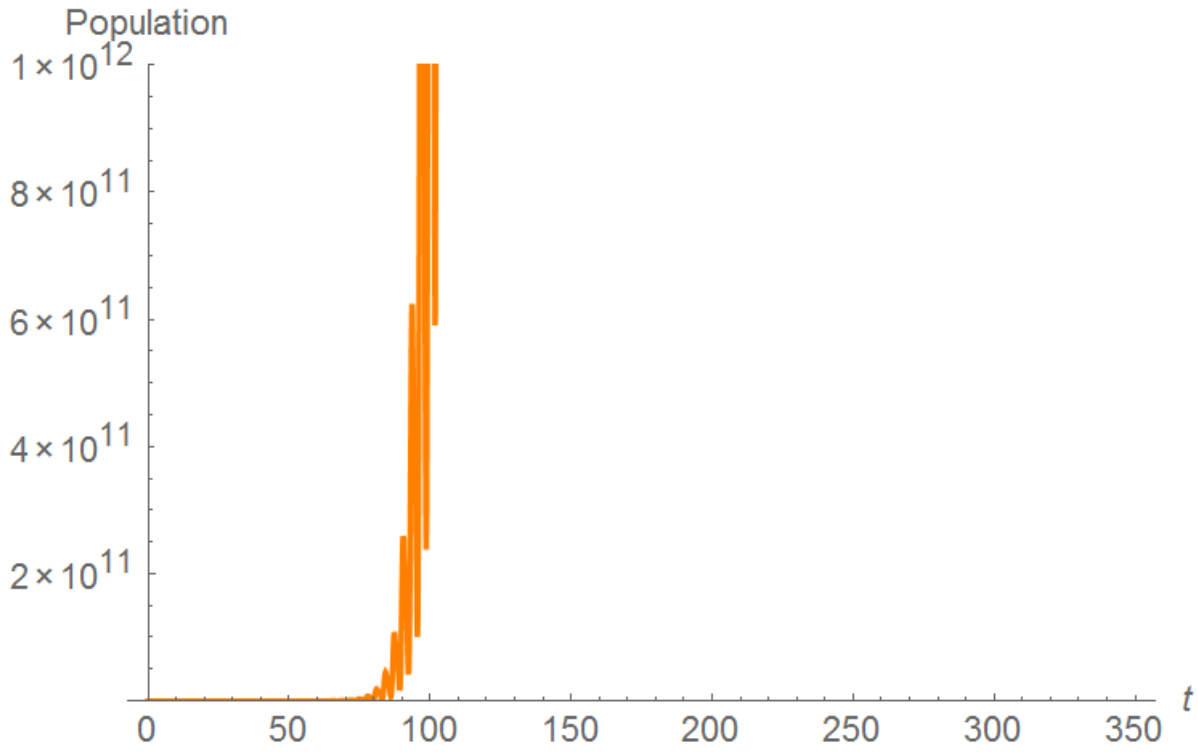

Figure 8a Plot of Generalized Rabi oscillation for Hamiltonian. $\boldsymbol{H_1(t)}$ when $(\boldsymbol{\gamma = 2, \mu = 1.95})$ via populations of spin up.

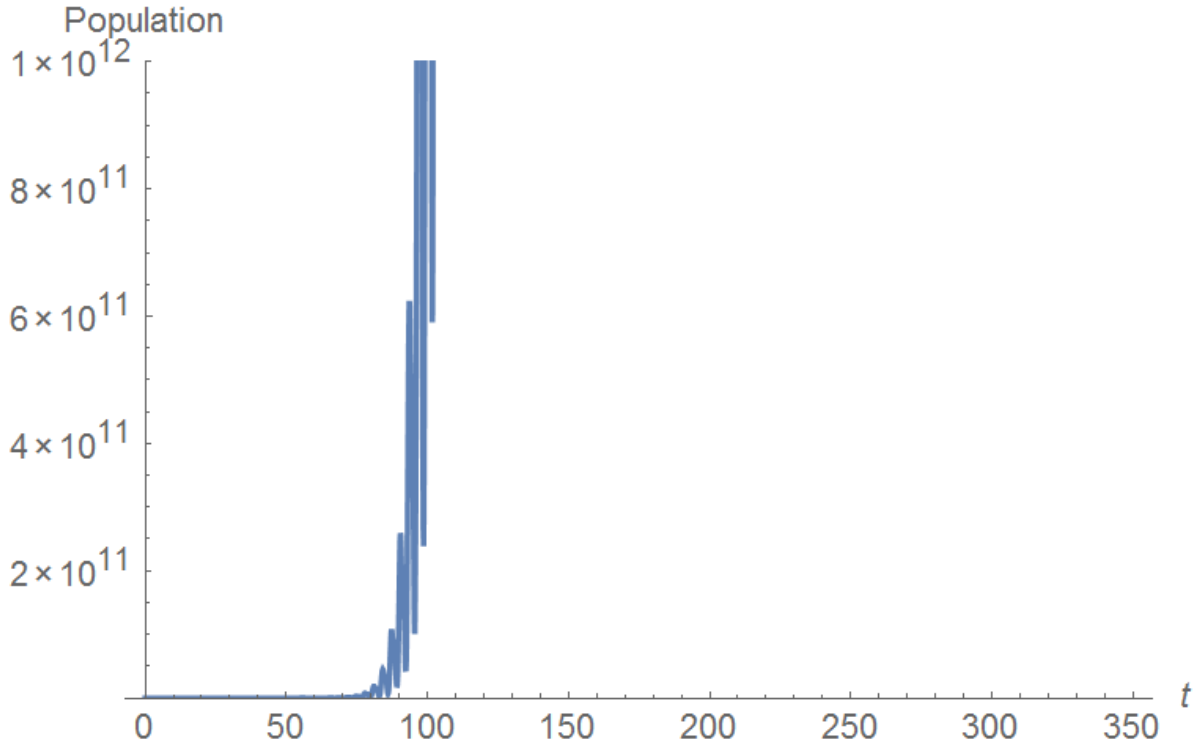

Figure 8b Plot of Generalized Rabi oscillation for Hamiltonian. $\boldsymbol{H_1(t)}$ when $(\boldsymbol{\gamma = 2, \mu = 1.95})$ via populations of spin down.

However, when extended unitarity is present such as the case where $(\gamma = 2, \mu = 2.05)$, we can observe immediately from Figure 9a and 9b that the population oscillation of the system from an initial up-state is stable, coherent and periodic. This therefore shows that once we are in the domain of extended unitarity, we can conclude that the periodic driving is capable of stabilizing the non-Hermitian system. Since this type of oscillation is a more general form of Rabi oscillation, we termed it as "Generalized Rabi oscillation".

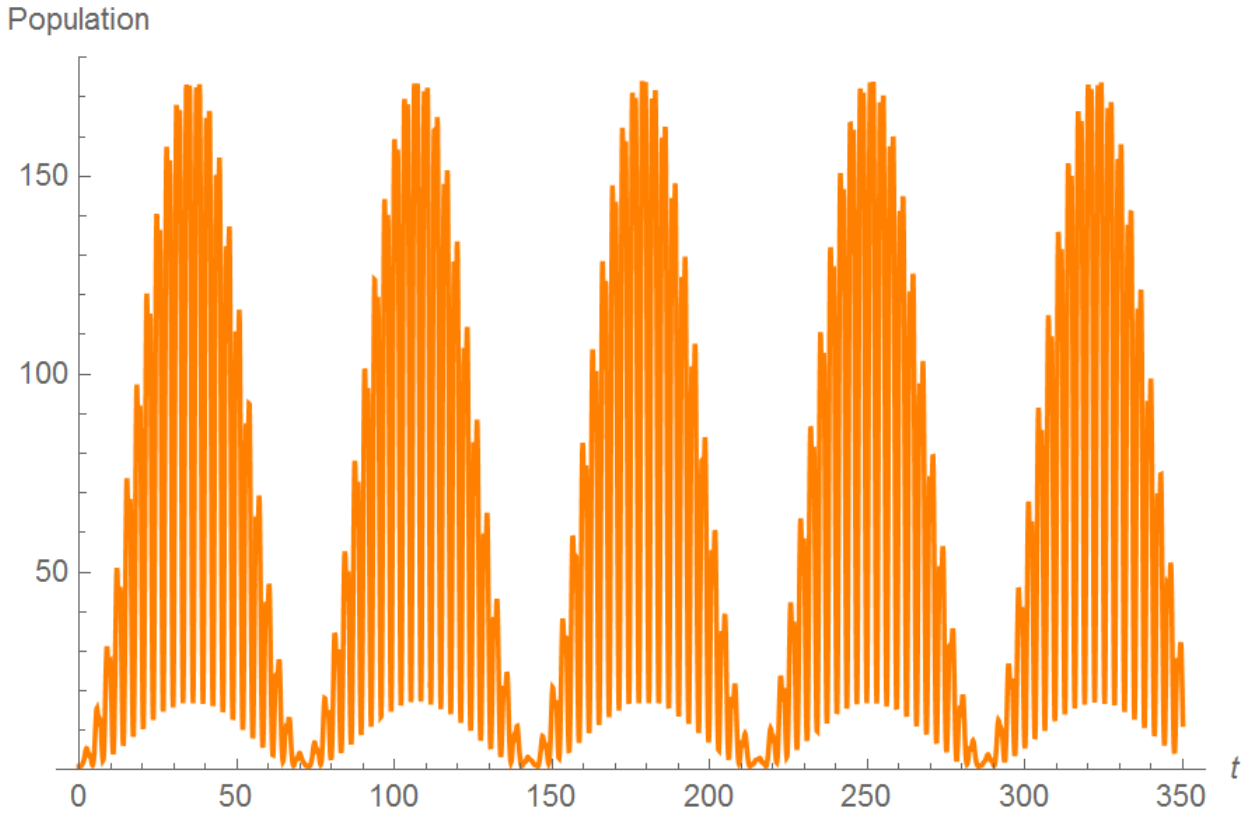

Figure 9a Plot of Generalized Rabi oscillation for Hamiltonian. $\boldsymbol{H_1(t)}$ when $(\boldsymbol{\gamma = 2, \mu = 2.05})$ via populations of spin up.

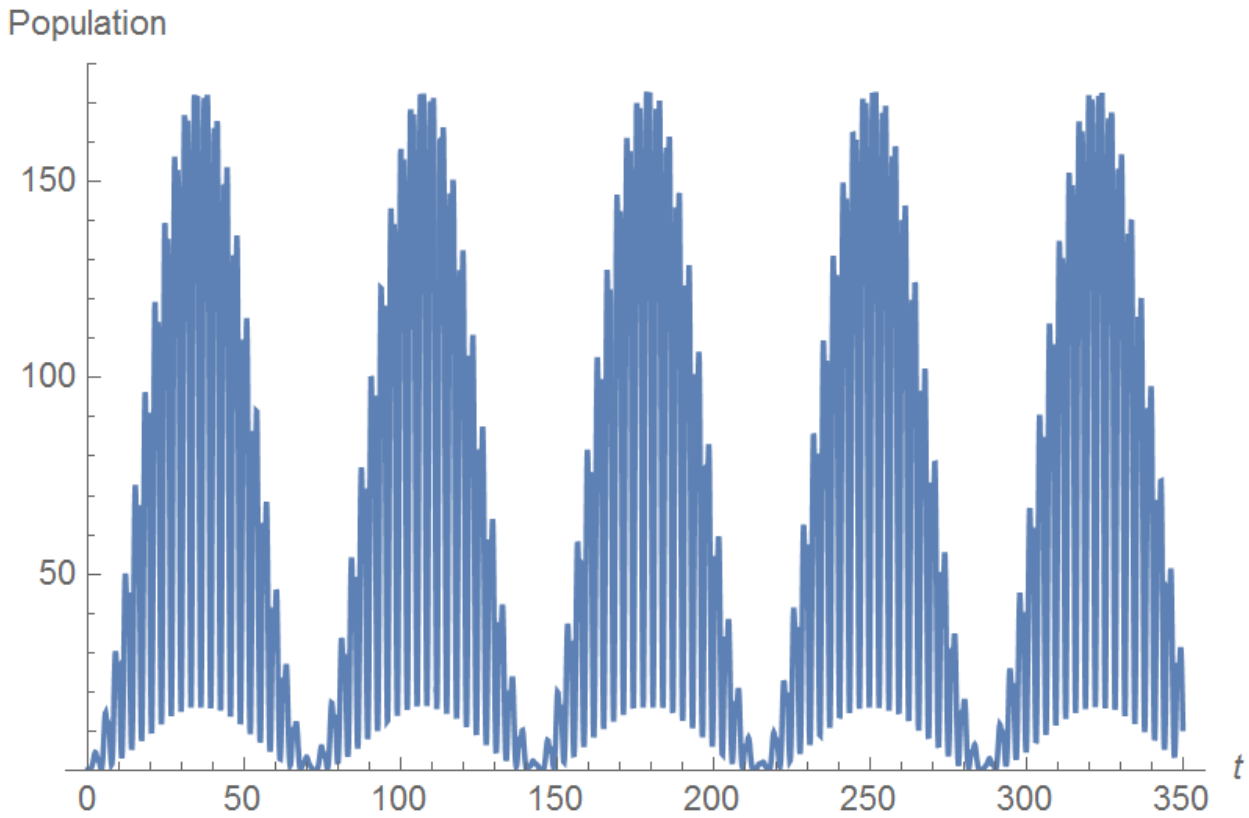

Figure 9b Plot of Generalized Rabi oscillation for Hamiltonian. $\boldsymbol{H_1(t)}$ when $(\boldsymbol{\gamma = 2, \mu = 2.05})$ via populations of spin down.

On the other hand, even though we have got a stabilized system, we do notice that the total population of the 2 states going beyond unity (non-norm-preserving) instead of being confined to unity just like the case of a Hermitian Hamiltonian in Chapter 2. We should however not be alarmed by this result because as illustrated in earlier chapters, we know that the purpose of introducing non-Hermitian Hamiltonian is to describe physical phenomena that involves gain and loss i.e. an open system. Since the system that is involved is open, we should undoubtedly expect that the total population of the 2 states to go beyond unity. In contrast, in chapter 2, the system under consideration is a closed system, thus, having a norm-preserving oscillation is an expected result.

7.2 Dynamical study of Hamiltonian, $\boldsymbol{H_3(t)}$

In order to verify that such generalized Rabi oscillation is coherent for any periodic driving field instead of a purely sinusoidal one, similar dynamical study is done on $H_3(t)$ as well

at $(\gamma = 0.2, \mu = 0.4)$ (satisfy extended unitarity) and $(\gamma = 0.2, \mu = 1.2)$ (Do not satisfy extended unitarity). Upon performing a population calculation for both cases, the following plots as shown in Figure 10, 11a and 11b are being obtained.

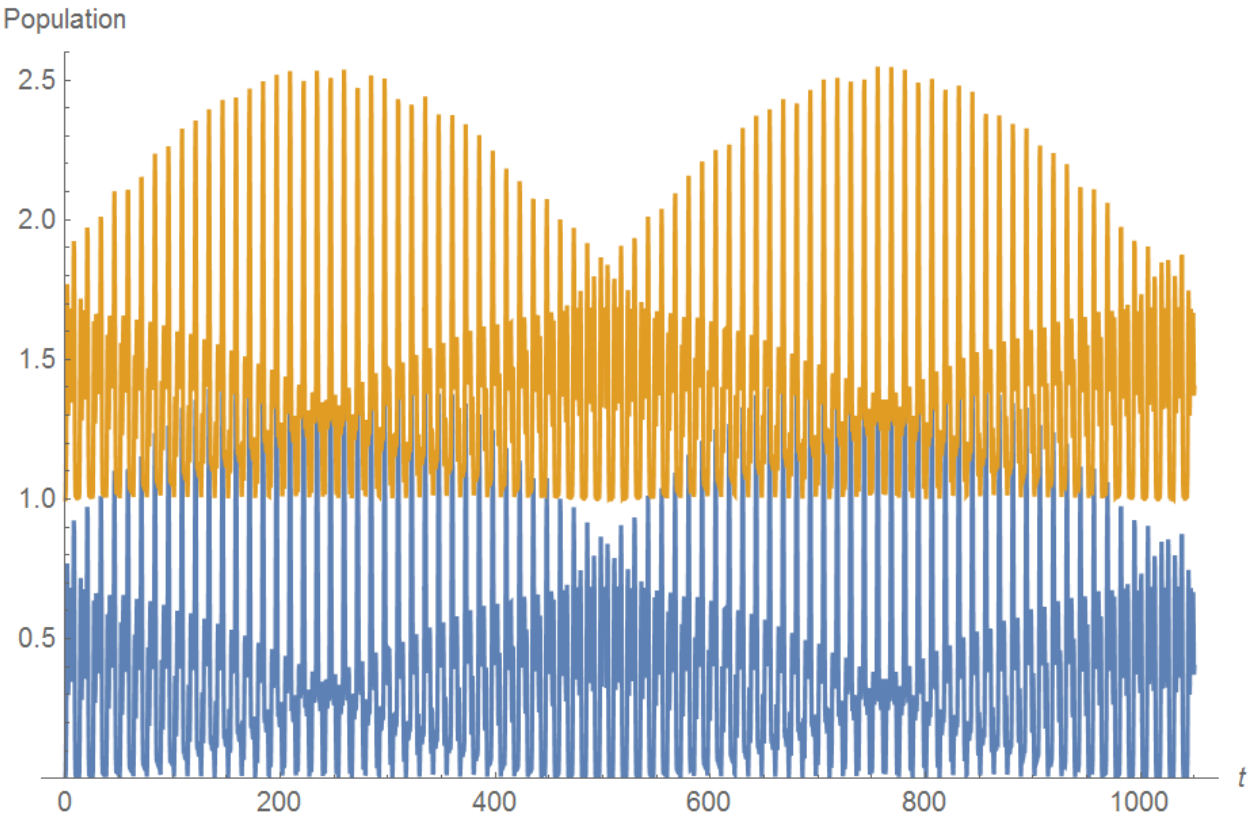

Figure 10 Plot of Generalized Rabi oscillation for Hamiltonian. $\boldsymbol{H_3(t)}$ when$(\boldsymbol{\gamma = 0.2, \mu = 0.4})$ via populations of spin down (Blue line) and for populations of spin up (Orange line).

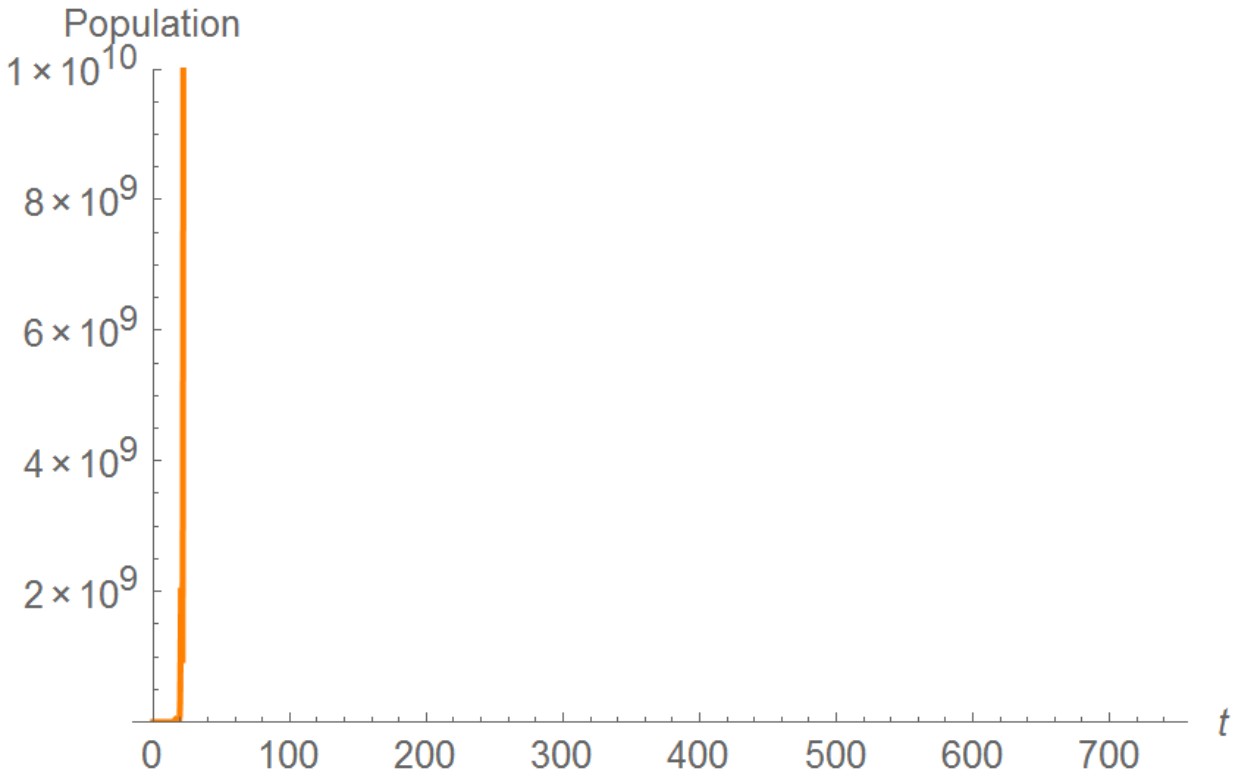

Figure 11a Plot of Generalized Rabi oscillation for Hamiltonian. $\boldsymbol{H_3(t)}$ when $(\boldsymbol{\gamma = 0.2, \mu = 1.2})$ via populations of spin up.

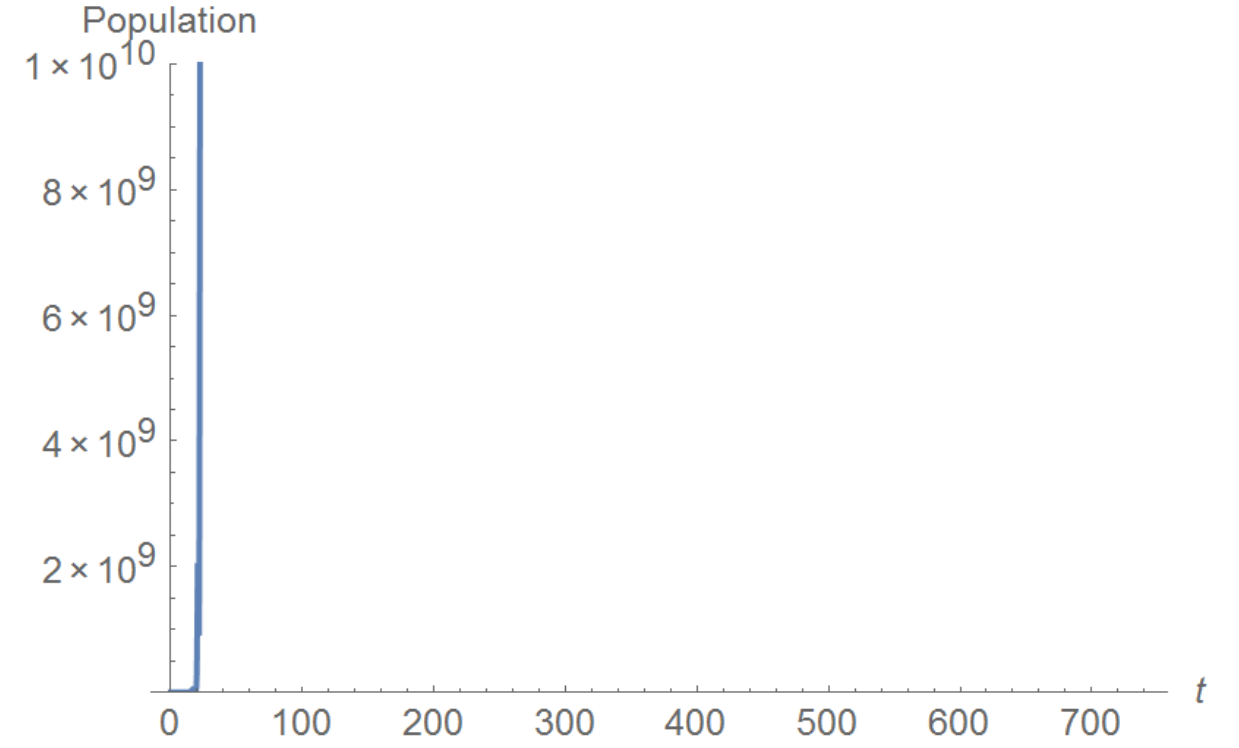

Figure 11b Plot of Generalized Rabi oscillation for Hamiltonian. $\boldsymbol{H_3(t)}$ when $(\boldsymbol{\gamma = 0.2, \mu = 1.2})$ via populations of spin down.

Once again, we see from Figure 10 that for the case whereby extended unitarity conditions are being satisfied, there is a stable, coherent and periodic Generalized Rabi oscillation for the population of both states. This shows that the system is being stabilized despite being driven by a non-sinusoidal periodic driving field. Similarly, the Generalized Rabi oscillations are also non-norm-preserving as expected because the non-Hermitian Hamiltonian $H_3(t)$ also describes an open system as well.

On the other hand, when we are in the domain where extended unitarity is absent, the population of the system blows up quickly and become unstable after a few period of driving as shown in Figure 11a and 11b. This thus shows that it is the absence of extended unitarity that resulted in the unstable evolution of a non-Hermitian system and not attributing the reason of instability to not having a perfectly sinusoidal driving field.

With this, we come to a conclusion and affirmation of section 6.3 that the crucial factor that ensures the stabilization of a non-Hermitian system is whether extended unitarity condition are being satisfied by the periodic driving field or not. It is not necessary for the driving field to be perfectly sinusoidal in order to stabilize a non-Hermitian system.

Chapter 8

2 Qubit System Interactions

8.1 Extended Unitarity for a 2 Qubit system

After handling various two-level systems in the preceding chapters, we are also interested in studying whether such stabilization of system is possible for a 2 qubit system. Consider the following system:

$$H_4(t) = \left\{\gamma\, \sigma_z^{(1)} + i\mu\, sin(t)\, \sigma_x^{(1)}\right\} \otimes I^{(2)} + I^{(1)} \otimes \epsilon\, \sigma_z^{(2)} + J\{\sigma_x^{(1)} \otimes \sigma_x^{(2)}\}$$

which is a system of 2 qubits that comprise of the non-Hermitian periodically driven Hamiltonian, $H_1(t)$ for the first system, a static Hamiltonian for the second system and also an interaction term with magnitude J between the two systems that is given by the last term.

By expanding them explicitly, we get $H_4(t)$ as follow,

$$H_4(t) = \begin{pmatrix} -\gamma + \epsilon & 0 & i\mu\sin(t) & J \\ 0 & -\gamma - \epsilon & J & i\mu\sin(t) \\ i\mu\sin(t) & J & \gamma + \epsilon & 0 \\ J & i\mu\sin(t) & 0 & \gamma - \epsilon \end{pmatrix}$$

Due to the difficulties in producing a high dimensional phase diagram here for a system parameterized by 4 different parameters, we begin with studying the case where $J = 1, \epsilon = 1$ and scan for the domains in which γ and μ gives us the condition of extended unitarity. Upon perform the evaluation using Mathematica, a phase diagram is being obtained and shown in Figure 12.

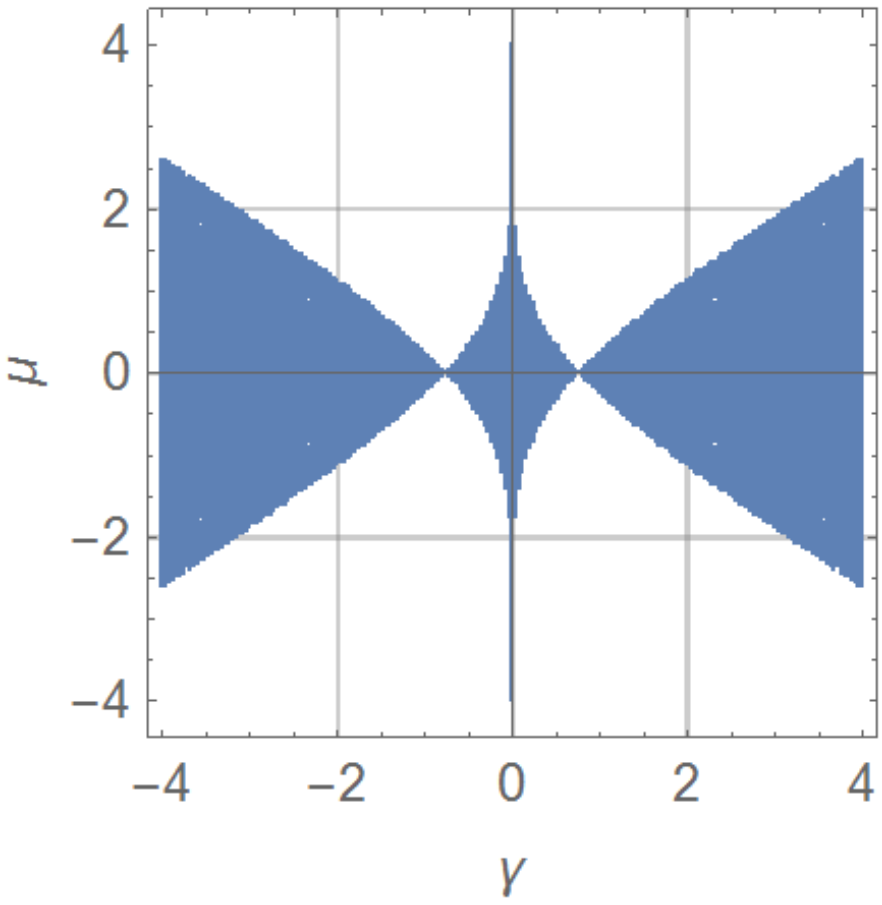

Figure 12 Phase Diagram for parameters $\boldsymbol{\gamma}, \boldsymbol{\mu}$ for Hamiltonian, $\boldsymbol{H_4(t)}$ and $\boldsymbol{J = 1, \epsilon = 1}$. Shaded regions are domains of $\boldsymbol{\gamma}, \boldsymbol{\mu}$ whereby extended unitarity condition is fulfilled.

Upon analyzing the phase diagram, we see that even for the case of a 2 qubit system, there are still domains of (γ, μ) where extended unitarity is present. This therefore shows us that it is *possible to generalize our idea of extended unitarity to multiple qubits system that is periodically driven as well.*

8.2 Generalized Rabi Oscillation for a 2 Qubit system

In this section we can go on to study the dynamics of the system via the use of generalized Rabi oscillation of the 2 qubit system described above. Specifically for the case where $J = 1, \epsilon = 1$, a population calculation is being performed in the domain where extended unitarity is present and the population dynamics are being compared with that in the domains whereby extended unitarity is absent.

To illustrate this, we study the point where $(\gamma, \mu) = (3,1)$. It can be easily seen from Figure 12 that this point lies within the domain where extended unitarity is present. A population calculation similar to that described in chapter 7 is being performed for $H_4(t)$ with an initial state where $|\Psi(t_0)\rangle = (1,0,0,0)$. By doing so, we will be able to see graphically from Figure 13 how the population of the system $(i.e. |a(t)|^2, |b(t)|^2, |c(t)|^2, |d(t)|^2)$ evolves with time whereby $|\Psi(t)\rangle = (a(t), b(t), c(t), d(t))$.

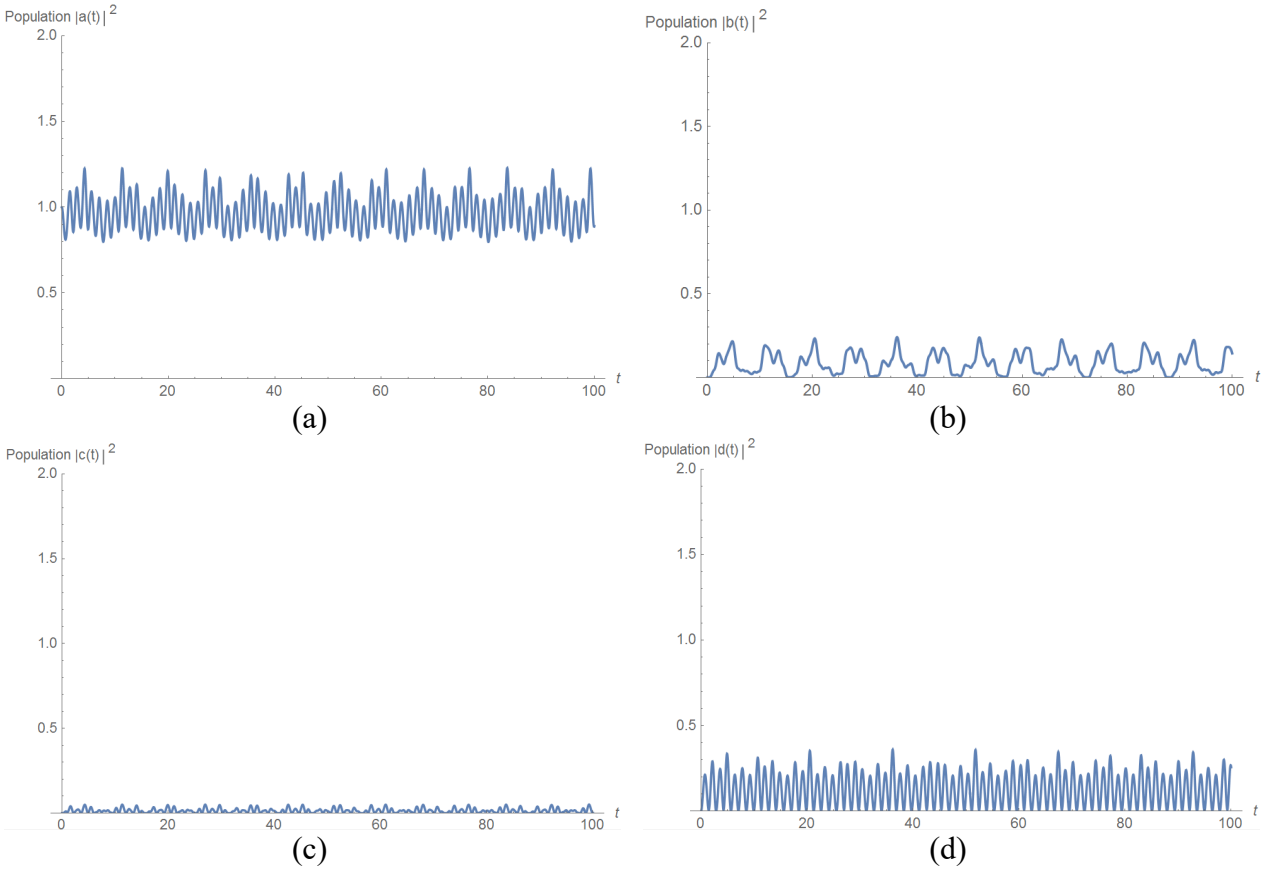

Figure 13 Plot of Generalized Rabi oscillations for Hamiltonian. $\boldsymbol{H_4(t)}$ for $(\boldsymbol{\gamma = 3, \mu = 1, J = 1, \epsilon = 1})$ (a)$\boldsymbol{|a(t)|^2}$ vs $\boldsymbol{t}$, (b)$\boldsymbol{|b(t)|^2}$ vs $\boldsymbol{t}$, (c)$\boldsymbol{|c(t)|^2}$ vs $\boldsymbol{t}$, (d)$\boldsymbol{|d(t)|^2}$ vs $\boldsymbol{t}$.

Once again we see a stable and coherent generalized Rabi oscillation for the case where extended unitarity condition is being fulfilled for the 2 qubit system. Furthermore, we can observe from Figure 13 easily that even though stabilization of the system is being achieved, the total population of the states also goes beyond unity similar to the case in chapter 7. This is an expected result as well because $H_4(t)$ is a non-Hermitian Hamiltonian that describes an open system. Therefore we should expect that the total population of the system to go beyond unity.

Now, we go on to study the case where $(\gamma, \mu) = (3,3)$. It can also be easily observed from Figure 12 that this point lies in the domain whereby extended unitarity is absent. After performing a population calculation at these system parameters, we observed in Figure 14 that the population of the system "blows up" exponentially after just a few period of driving. This is an expected result as well because these values of (γ, μ) do not fulfill extended unitarity condition.

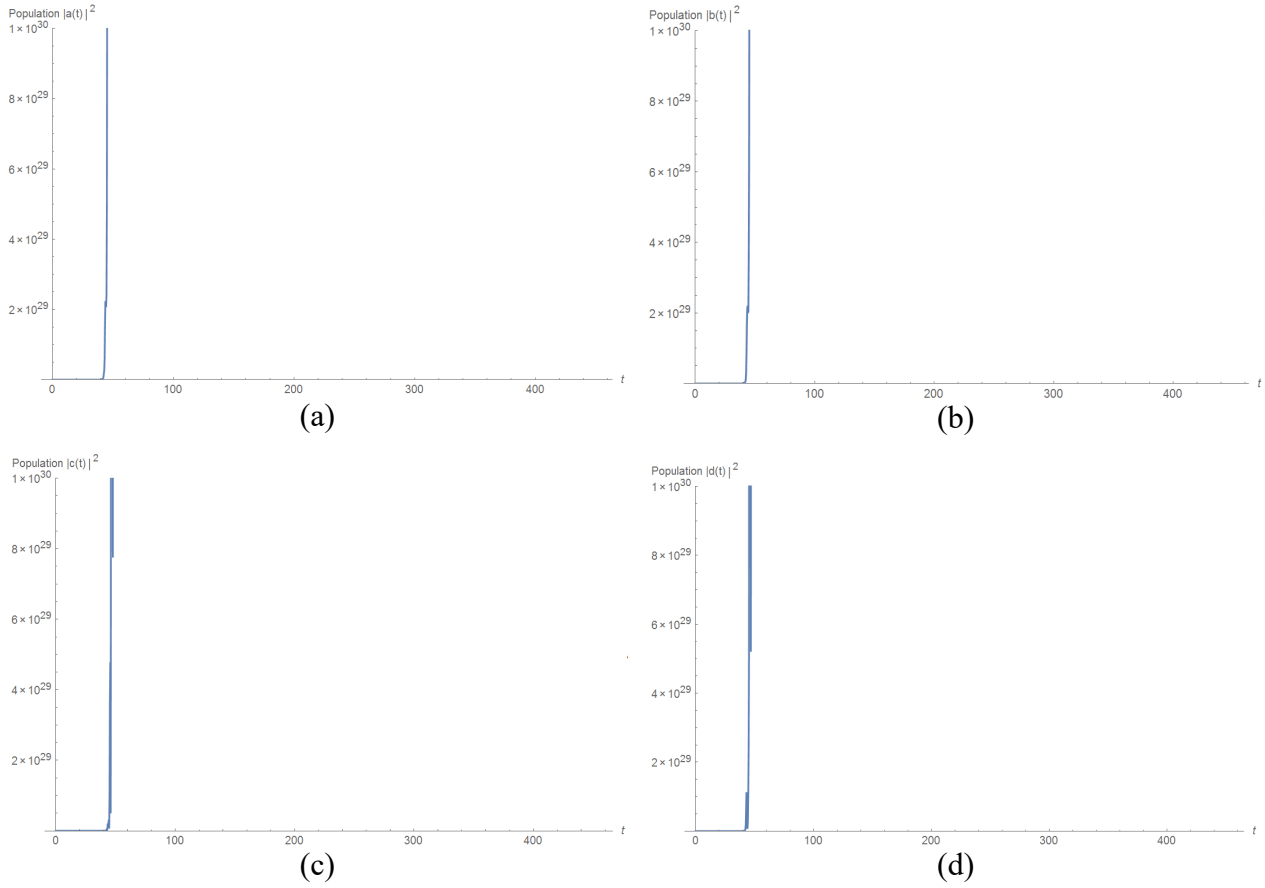

Figure 14 Plot of Generalized Rabi oscillations for Hamiltonian. $\boldsymbol{H_4(t)}$ for $(\boldsymbol{\gamma = 3, \mu = 3, J = 1, \epsilon = 1})$ (a)$|\boldsymbol{a(t)}|^2$ vs $\boldsymbol{t}$, (b)$|\boldsymbol{b(t)}|^2$ vs $\boldsymbol{t}$, (c)$|\boldsymbol{c(t)}|^2$ vs $\boldsymbol{t}$, (d)$|\boldsymbol{d(t)}|^2$ vs $\boldsymbol{t}$.

Given all these results that concur with the case of a single qubit system, we can therefore *conclude that our idea of Generalized Rabi oscillation can be extended to include system where 2 or more qubit systems interacts. Furthermore, we can also conclude that for a 2 qubit system, it is also true that at domains where extended unitarity is present, stabilization of the non-Hermitian system is possible via periodic driving and vice versa.*

8.3 Varying ϵ and interaction strength, J

Similar to the manipulation that was done in section 6.2, we can vary the third parameter to see how whether extended unitarity emerges when other parameters are being varied.

Varying $\epsilon = 2, 3, 4$ with $J = 1$

First of all, by varying the energy difference, ϵ of the 2 states in the second non-driven system from $\epsilon = 2,3,4$ with $J = 1$, we see that extended unitarity condition is still being fulfilled at well-defined domains of (γ, μ) as shown in Figure 15a to 15c**.** These results also concur with results from section 6.2 whereby varying a third parameter still allows extended unitarity to emerge even in a 2 qubit system. Furthermore, it is also interesting to see that from Figure 15c when $\epsilon = 4$, the phase diagram return back to the same one as obtained in Figure 3 by $H_1(t)$ alone. It is as if the 2 qubit system can now be treated as if it is a single qubit system. It would be interesting to study the specific values of J and ϵ such that the above phenomenon can occur and even check if the further increment of ϵ will lead to a periodic evolution of the phase diagrams.

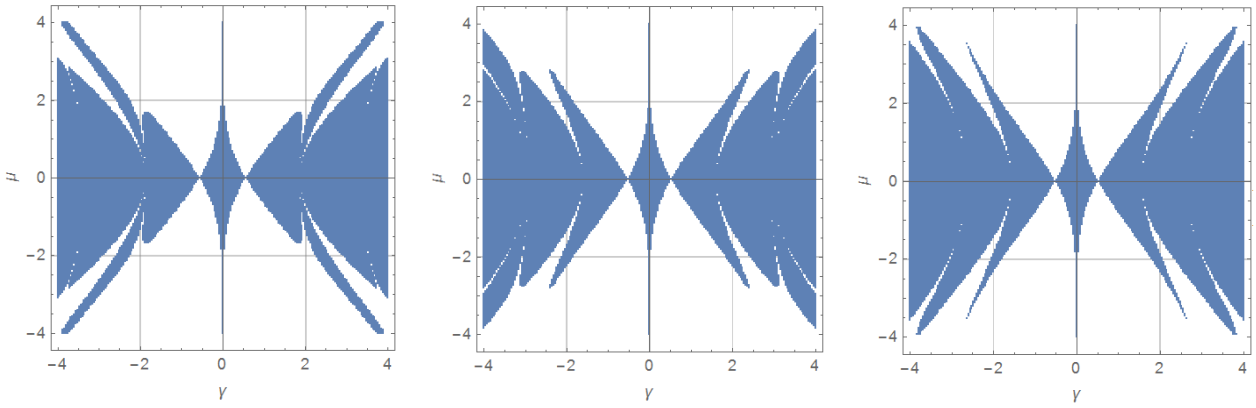

(a) (b) (c)

Figure 15 Phase diagram for parameters γ, μ for Hamiltonian, $H_4(t)$ with varying ϵ (a) $\epsilon = 2$, (b) $\epsilon = 3$ and (c) $\epsilon = 4$ and constant $J = 1$. Shaded regions are domains of γ, μ whereby extended unitarity condition is fulfilled.

Varying $J = 2, 3, 4$ with $\epsilon = 1$

As for the case where the interaction strength, J is being varied while keeping $\epsilon = 1$, we see that when the interaction strength, J increases from 1 to 4, the number of domains (Areas shaded in blue in Figure 16a to 16c) that fulfill extended unitarity condition actually decreases. This therefore shows that there are now fewer domains of γ and μ in the range $-4 \leq \gamma \leq 4$ and $-4 \leq \mu \leq 4$ which allow stabilization of the non-Hermitian system by periodic driving. This is

in contrast to naïve thinking that increasing interaction strength will increase the domains for system stabilization. Instead, increasing interaction strength actually decreases the domains of (γ, μ) that gives us a stabilized system via periodic driving for this case. One should also take note that when the interaction strength goes towards zero, the interaction between the 2 qubit system get less and less significant until they no longer interact when $J = 0$. When this happens we should obtain a phase diagram that is similar to Figure 3 as if the presence of the second system is of no relevance to the first.

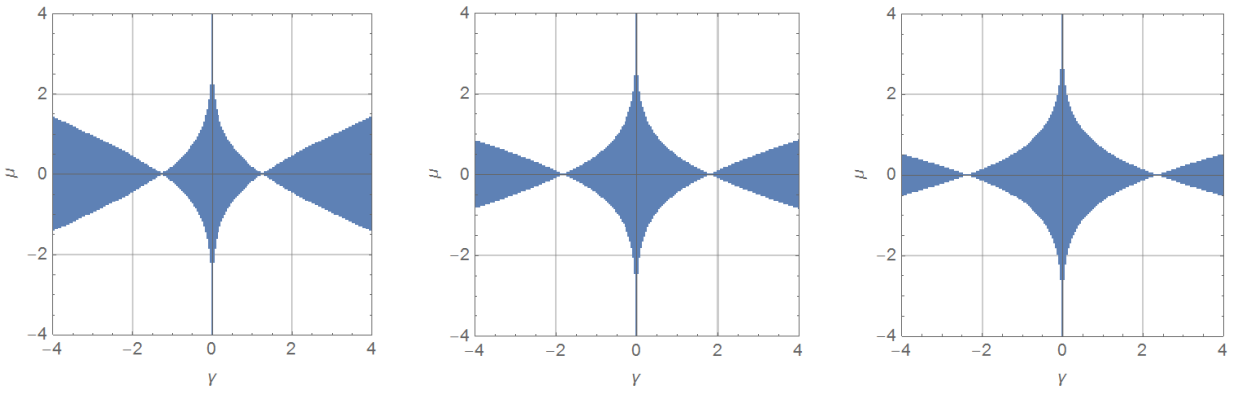

(a) (b) (c)

Figure 16 Phase diagram for parameters γ, μ for Hamiltonian, $H_4(t)$ with varying J (a) $J = 2$, (b) $J = 3$ and (c) $J = 4$ and constant $\epsilon = 1$. Shaded regions are domains of γ, μ whereby extended unitarity condition is fulfilled.

Therefore, we can conclude that the variation of a third parameter to a 2 qubit system still allow for extended unitarity to emerge. This thus makes stabilization of the non-Hermitian system possible via the use of periodic driving. Lastly, after studying about the concept of extended unitarity and stabilization of a 2 qubit system via periodic driving in this chapter, it would be interesting for future research to extend the concept to *N* qubit system and verify that the concept is true in general.

Chapter 9

Mapping to a Band Structure Problem

In this chapter, following Gong. and Wang.'s paper [5] we are going to discuss on how to map the problem of stabilizing a driven non-Hermitian system into a band structure problem. This is because the band structure problem is a very common problem in the realm of Solid State Physics and it would be interesting to see how our concept of extended unitarity is related to it. First, let us consider the following general Hamiltonian:

$$H(t) = [a\vec{\boldsymbol{n}}_{\boldsymbol{3}} + ib(t)\vec{\boldsymbol{n}}_{\boldsymbol{1}}] \cdot \vec{\boldsymbol{\sigma}}$$

where a is a time independent constant, $b(t) = b(t+T)$ is a complex periodic function with respect to time, $\{\vec{\boldsymbol{n}}_1, \vec{\boldsymbol{n}}_{\boldsymbol{2}}, \vec{\boldsymbol{n}}_{\boldsymbol{3}}\}$ is an arbitrary fixed set of right-handed basis and $\vec{\boldsymbol{\sigma}} = (\sigma_x, \sigma_y, \sigma_z)$ the Pauli vector. It is also clear that the above Hamiltonian for a two-level system is traceless and non-Hermitian in nature. To make our analysis simpler, we let

$$\{\vec{\boldsymbol{n}}_{\boldsymbol{1}}, \vec{\boldsymbol{n}}_{\boldsymbol{2}}, \vec{\boldsymbol{n}}_{\boldsymbol{3}}\} = \left\{\begin{pmatrix}1\\0\\0\end{pmatrix}, \begin{pmatrix}0\\1\\0\end{pmatrix}, \begin{pmatrix}0\\0\\1\end{pmatrix}\right\}$$

As a result, the Hamiltonian becomes:

$$H(t) = a\sigma_z + ib(t)\sigma_x = \begin{pmatrix} a & ib(t) \\ ib(t) & -a \end{pmatrix}$$

which is very similar to the basic Hamiltonian introduced in Chapter 6. Furthermore, we also assume a^2 to be real for reasons that will be illustrated later. Since the Hamiltonian is being expanded in the Pauli basis, we will expand the time-evolution operator, $U(t,0)$ in the same representation as well, yielding:

$$U(t,0) = \boldsymbol{I}\, u_0(t) + \sum_{i=1}^{3} u_i(t)\vec{\boldsymbol{n}}_{\boldsymbol{i}} \cdot \vec{\boldsymbol{\sigma}}$$

In the simplified version,

$$U(t,0) = u_0 \begin{pmatrix}1 & 0\\0 & 1\end{pmatrix} + u_1 \begin{pmatrix}0 & 1\\1 & 0\end{pmatrix} + u_2 \begin{pmatrix}0 & -i\\i & 0\end{pmatrix} + u_3 \begin{pmatrix}1 & 0\\0 & -1\end{pmatrix}$$
$$= \begin{pmatrix} u_0 + u_3 & u_1 - iu_2 \\ u_1 + iu_2 & u_0 - u_3 \end{pmatrix}$$

To make the expression tidier, we note that $u_i(t)$ is dependent on t and we shall drop the parenthesis, (t) as we did for the expression above and only express it when necessary.

Eigenvalues of $U(t,0)$, λ are also being evaluated as follow:

$$Det[U(t,0) - I\lambda] = 0$$

$$\begin{vmatrix} (u_0 + u_3) - \lambda & u_1 - iu_2 \\ u_1 + iu_2 & (u_0 - u_3) - \lambda \end{vmatrix} = 0$$

$$u_0^2 - u_3^2 - 2u_0\lambda + \lambda^2 - u_1^2 - u_2^2 = 0$$

$$\lambda^2 - 2u_0\lambda + (u_0^2 - u_1^2 - u_2^2 - u_3^2) = 0$$

$$\lambda_\pm = \frac{2u_0 \pm \sqrt{4u_0^2 - 4u_0^2 + 4u_1^2 + 4u_2^2 + 4u_3^2}}{2} = u_0 \pm \sqrt{u_1^2 + u_2^2 + u_3^2}$$

From Appendix B it is understood that the determinant of the Floquet operator needs to be at unity, therefore, we shall write $\lambda_\pm$ in its real and imaginary form for reasons that will be clear later.

$$Det[U(T,0)] = 1$$

$$\begin{vmatrix} u_0 + u_3 & u_1 - iu_2 \\ u_1 + iu_2 & u_0 - u_3 \end{vmatrix} = 1$$

$$u_0^2 - u_1^2 - u_2^2 - u_3^2 = 1$$

$$u_0^2 - 1 = u_1^2 + u_2^2 + u_3^2$$

$$\therefore \lambda_\pm = u_0(T) \pm \sqrt{u_0^2(T) - 1} = u_0(T) \pm i\sqrt{1 - u_0^2(T)}$$

Using Euler's Formula, we can write $\lambda_\pm$ in the following form,

$$e^{\pm i\beta} = u_0(T) \pm i\sqrt{1 - u_0^2(T)}$$

$$= cos(\beta) \pm i\, sin(\beta)$$

In this form, we can see that to satisfy extended unitarity condition, β need to be real eigenphases. Therefore, we only need to fulfill the condition of $-1 \leq u_0(T) \leq 1$. This will thus gives $\beta = \cos^{-1}(u_0(T))$ as the solution for the eigenphases. It is also understood that after N periods of evolution, the Floquet operator will become $U(NT,0)$ with eigenvalues of $e^{\pm iN\beta}$. This will therefore lead us easily to the more general condition of $-1 \leq u_0(NT) \leq 1$ in order for extended unitarity condition to be fulfilled.

Since we have the explicit expression of all the required terms, we can write down the time-dependent Schrödinger equation explicitly.

Setting $\hbar = 1$,

$$i\frac{d}{dt}U(t,0) = H(t)U(t,0)$$

$$i\frac{d}{dt}\begin{pmatrix} u_0+u_3 & u_1-iu_2 \\ u_1+iu_2 & u_0-u_3 \end{pmatrix} = \begin{pmatrix} a & ib(t) \\ ib(t) & -a \end{pmatrix}\begin{pmatrix} u_0+u_3 & u_1-iu_2 \\ u_1+iu_2 & u_0-u_3 \end{pmatrix}$$

Upon simplifying as shown in Appendix D, we obtained 4 equations as follow:

$$\begin{cases} \dot{u}_0(t) = b(t)u_1(t) - iau_3(t) \\ \dot{u}_1(t) = b(t)u_0(t) - au_2(t) \\ \dot{u}_2(t) = au_1(t) - ib(t)u_3(t) \\ \dot{u}_3(t) = -iau_0(t) + ib(t)u_2(t) \end{cases} \tag{9.1}$$

In order to decouple the equations, equation (9.1) is differentiated with respect to t. After which some cancellation of the 1st order derivatives of $u_i(t)$ is being performed yielding us the following:

$$\begin{cases} \ddot{u}_0(t) = [b^2(t) - a^2]u_0(t) + \dot{b}(t)u_1(t) \\ \ddot{u}_1(t) = \dot{b}(t)u_0(t) + [b^2(t) - a^2]u_1(t) \\ \ddot{u}_2(t) = -i\dot{b}(t)u_3(t) + [b^2(t) - a^2]u_2(t) \\ \ddot{u}_3(t) = i\dot{b}(t)u_2(t) + [b^2(t) - a^2]u_3(t) \end{cases}$$

By some clever observation, the above can be written down in the matrix form as below.

$$\left[-\frac{d^2}{dt^2}\begin{pmatrix} 1 & 0 & 0 & 0 \\ 0 & 1 & 0 & 0 \\ 0 & 0 & 1 & 0 \\ 0 & 0 & 0 & 1 \end{pmatrix} + \begin{pmatrix} b^2(t) & \dot{b}(t) & 0 & 0 \\ \dot{b}(t) & b^2(t) & 0 & 0 \\ 0 & 0 & b^2(t) & -i\dot{b}(t) \\ 0 & 0 & i\dot{b}(t) & b^2(t) \end{pmatrix}\right]\begin{pmatrix} u_0(t) \\ u_1(t) \\ u_2(t) \\ u_3(t) \end{pmatrix} = a^2\begin{pmatrix} u_0(t) \\ u_1(t) \\ u_2(t) \\ u_3(t) \end{pmatrix}$$

To map the above matrix equation into a band structure equation, we map our time variable, t onto a space variable, x. Furthermore, we can decouple the above matrix equation into two separate eigenvalue equations for a band structure problem with identical spectra by introducing the following wavefunctions:

$$\Psi(x) = A\begin{pmatrix} u_0(x) \\ u_1(x) \end{pmatrix} \quad \text{and} \quad \Phi(x) = A\begin{pmatrix} u_2(x) \\ u_3(x) \end{pmatrix}$$

with A as an arbitrary constant, giving us:

$$\left[-\frac{d^2}{dx^2} + b^2(x) + \frac{db(x)}{dx}\sigma_x\right]\Psi(x) = a^2\Psi(x)$$

$$\left[-\frac{d^2}{dx^2}+b^2(x)+\frac{db(x)}{dx}\sigma_y\right]\Phi(\mathrm{x})=\mathrm{a}^2\Phi(x)$$

To simply these expressions even further, we see that if we define:

$$\psi^{\pm}(x)=A[u_0(x)\pm u_1(x)] \qquad \text{and} \qquad \phi^{\pm}(x)=A[u_2(t)\mp iu_3(x)]$$

as the Bloch eigenfunctions, we can massage the equation into the following:

$$\left[-\frac{d^2}{dx^2}+V^{\pm}(x)\right]\psi^{\pm}(x)=a^2\psi^{\pm}(x) \tag{9.2}$$

$$\left[-\frac{d^2}{dx^2}+V^{\pm}(x)\right]\phi^{\pm}(x)=a^2\phi^{\pm}(x) \tag{9.3}$$

where

$$V^{\pm}(x)=b^2(x)+\frac{db(x)}{dx} \tag{9.4}$$

By comparing the above with our time independent Schrödinger equation,

$$\left[-\frac{\hbar^2}{2m}\frac{d^2}{dx^2}+V(x)\right]\psi(x)=E\psi(x)$$

we can see that we have a system that is describing a particle with a mass of $\frac{1}{2}m$ moving in a periodic potential of $V^{\pm}(x)$. Since $V^{\pm}(x)$ is dependent on $b(t)$ which is a periodic function, $V^{\pm}(x)$ is also periodic in nature, having the same period, T as the driving field, $b(t)$, i.e. $V^{\pm}(x)=V^{\pm}(x+T)$.

With this, we have successfully mapped our time periodic driving problem into a band structure problem which is commonly tackled in the realm of solid state physics. To understand deeper the meaning of extended unitarity as introduced in Chapter 5 in this section, we remind ourselves that it arises when the condition $-1\leq u_0(NT)\leq 1$ is being fulfilled. Since we defined our Bloch eigenfunctions $\psi^{\pm}(x)$ and $\phi^{\pm}(x)$ earlier on which is made up of different linear combinations of $u_i(x)$, we see that for them to be the eigenfunctions for any potentials, $V(x)$, they must be "well-behaved". In particular, $\psi^{\pm}(x)$ and $\phi^{\pm}(x)$ should not go to infinity as $x\to\pm\infty$. This is not a problem when extended unitarity is satisfied (i.e. β are real eigenphases) because after N period evolution, where $x=NT$, $\psi^{\pm}(NT)=A[u_0(NT)\pm u_1(NT)]$ remains "well-behaved" by not growing exponentially. However, for the case where extended unitarity is absent (i.e. β are complex eigenphases) the condition where $-1\leq u_0(NT)\leq 1$ will no longer be valid. As a result, the supposedly Bloch eigenfunctions will diverge after N period evolutions.

This therefore makes them unsuitable as candidates to become true Bloch eigenfunctions. Thus, the problem of a periodically driven non-Hermitian Hamiltonian is being mapped successfully into a band structure problem. Furthermore, we can also see that because of this mapping being performed, we can interpret the real eigenphases, β of the Floquet operator, $U(T,0)$ as the product of the Bloch quasi-momentum and the lattice period in the band structure problem.

To see an example of how the mapping can be done, we can make use of Hamiltonian, $H_1(t)$. From $H_1(t)$, we can see without much difficulties that $\vec{\boldsymbol{n}}_{\boldsymbol{1}} = \hat{\boldsymbol{x}}, \vec{\boldsymbol{n}}_{\boldsymbol{3}} = \hat{\boldsymbol{z}}, a = \gamma$ and $b(t) = \mu\sin(t)$. Upon performing a mapping via the use of equation (9.4), we obtained $V_1^+(x) = \mu^2 \sin^2(t) + \mu\cos(t)$ as the mapped lattice potential. With these in hand, we are able to comprehend Figure 3 better and interpret the boundaries that separate the domains of extended unitarity as the presence of energy gaps for the lattice potential $V_1^+(x)$. Furthermore, the domains in which extended unitarity is present can also be interpreted as the values of all possible real band energy eigenvalues $a^2 = \gamma^2$ as a function of μ. A further check is also being performed by recording β when extended unitarity occurs for a particular value of μ for example $\mu = 0.1$. A plot of γ^2 against β is then plotted as shown in red squares in Figure 17. After which, a direct band structure calculations for $V_1^+(x)$ is also being performed and we obtain the following band dispersion relations which are being plotted using blue lines in Figure 17. Since we are able to obtain an exact match as shown in Figure 17, it verified that our mapping is indeed a correct one.

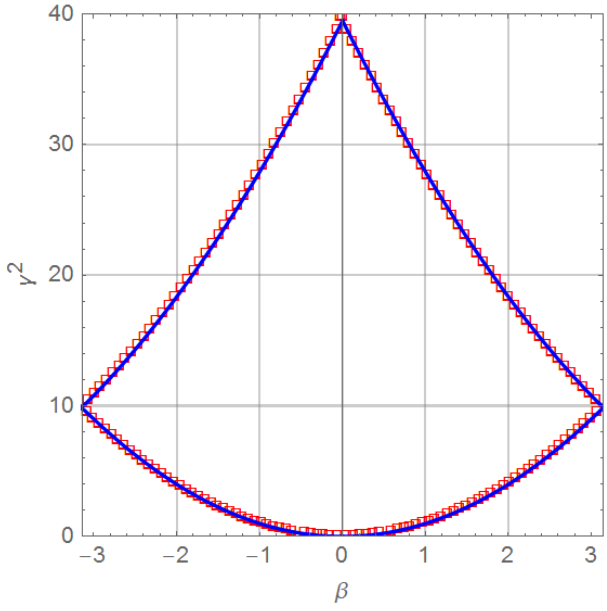

Figure 17 Identical dispersion relation obtained by direct band-structure calculations using $\boldsymbol{V_1^+(x)}$ (blue lines) or by checking for extended unitarity (red squares) when $\boldsymbol{\mu = 0.1}$.

Chapter 10

Comparison of Methods

In this chapter, we are going to compare the validity of our method of tackling the problem of stabilizing non-Hermitian system with the method that is being used in Yogesh et. al. research [39]. This is being done to demonstrate that given the same set of problem, we are able to tackle it using different approach and yet yield similar results. Lastly, we will compare the pros and cons of each method and appreciate the usefulness of each approach.

10.1 Method I: Checking of Floquet Hamiltonian's Eigenvalues

In a paper published by Yogesh et. al. in 2014 [39], a two-level system coupled to a non-Hermitian sinusoidal perturbing potential is being studied. This is being inspired by the recent research interest in studying Hamiltonians that are invariant under combined parity and time reversal conditions (PT-symmetry Quantum Mechanics). The Hamiltonian, H_0 studied in the paper is an *N*-site lattice with a constant tunneling, J and is perturbed by a periodic gain-loss potential $V(t)$ given by:

$$H_{Y,general} = H_0 + V(t)$$
$$= -\hbar J \sum_{x=1}^{N-1} (|x\rangle\langle x+1| + |x+1\rangle\langle x|) + i\hbar\gamma_Y \cos(\omega t)(|x_0\rangle\langle x_0| - |\bar{x}_0\rangle\langle \bar{x}_0|)$$

where $|x\rangle$ is the normalized state localized at x, the parity operator defined as $x \to \bar{x} = N + 1 - x$, $|x_0\rangle$ and $|\bar{x}_0\rangle$ are the loss or absorption sites depending on time, t. In the first part of his paper, a study on the above Hamiltonian on $N = 2$ is done and the general Hamiltonian reduces to equation (10.1).

$$H_Y(t) = i\hbar\gamma_Y \cos(\omega t)\, \sigma_z - \hbar J \sigma_x \tag{10.1}$$

Upon obtaining the 2 level Hamiltonian explicitly, Floquet theory is invoked to obtain the Floquet Hamiltonian. This is being done to find out where are domains in which the eigenspectrum (quasienergies) of the Floquet Hamiltonian are purely real. Yogesh and his team further define these domains as the phase where there is PT-symmetry whereas domains that result in the emergence of complex-conjugate in the eigenspectrum for the Floquet Hamiltonian

are termed as the PT-broken phase. An evaluation of the Floquet Hamiltonian gives us equation (10.2).

$$\left(H_{Y,F}\right)_{x,x'}^{p,q} =$$

$$p\hbar\omega\delta_{p,q}\delta_{x,x'} - \delta_{p,q}\hbar J\left(\delta_{x,x'+1} + \delta_{x,x'-1}\right) + \frac{i\hbar\gamma_Y}{2}\delta_{x,x'}(\delta_{p,q+1} + \delta_{p,q-1})(\delta_{x,\bar{x}_0} - \delta_{x,\bar{x}_0}) \quad (10.2)$$

where $p, q \in \mathbb{Z}$ denotes the Floquet band indices. Since the Floquet Hamiltonian is an infinite matrix, no computers are able to handle such numerical evaluation involving an infinite matrix. By defining $|p| \leq N_f$, and truncating the Floquet Hamiltonian at N_f will give us a $(2N_f + 1)N$-dimensional square matrix. The Floquet band cutoff $N_f \gg 1$ is also chosen so that results with cutoffs N_f and $2N_f$ are virtually identical, and thus remain valid in the limit $N_f \to \infty$ [40].

In view of this, Yogesh et. al. truncated the Floquet Hamiltonian at $N_f = 50$ and obtained a Floquet Hamiltonian of 101 bands. With this, an evaluation of the eigenspectrum (quasienergy) of the Floquet Hamiltonian in the domain: $\left(\frac{\gamma_Y}{J}, \frac{\omega}{J}\right)$ is being performed and a phase diagram that illustrates the strength of the imaginary component of the eigenspectrum with respect to the domain is being plotted in Figure18.

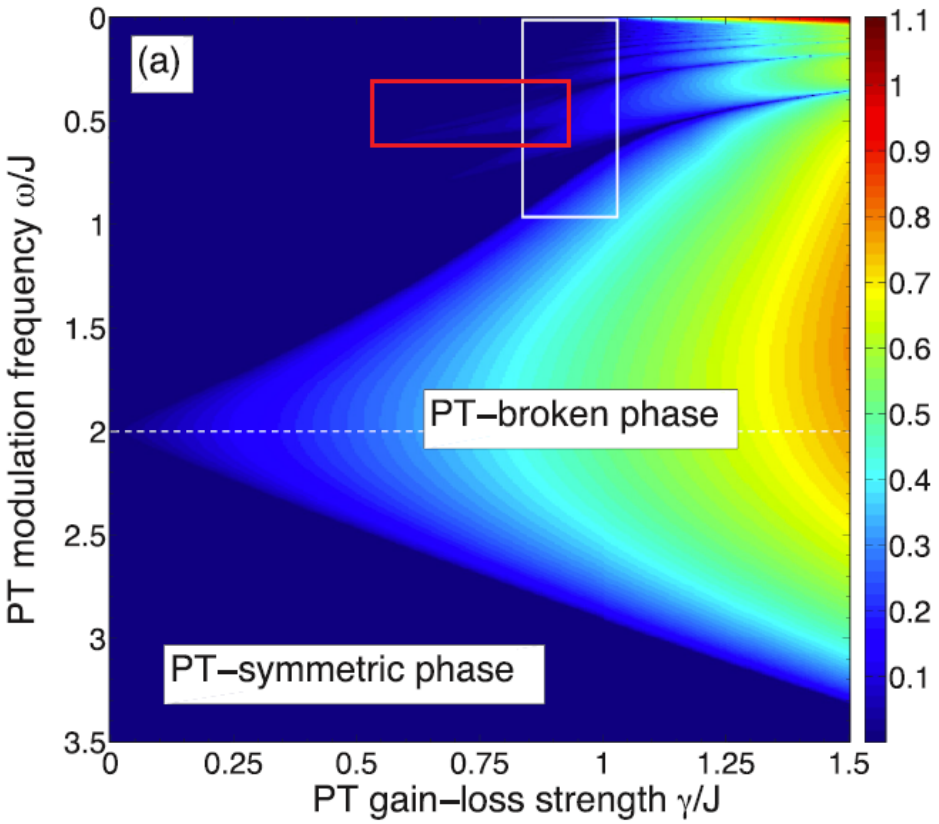

Figure 18 PT Phase diagram of a two-level system in the $(\boldsymbol{\gamma_Y}, \boldsymbol{\omega})$ plane described by $\boldsymbol{H_Y(t)}$. Plotted is the largest imaginery part of the spectrum of the Floquet Hamiltonian, $\boldsymbol{H_{Y,F}}$ obtained by Yogesh et.al [39]. Darkest blue region are domains where there is PT-symmetry i.e. Floquet quasienergies are real. Noises in the phase diagrams are highlighted using a red rectangle.

From Figure 18, the darkest blue regions are basically regions that are purely real while regions with other colours are domains where the imaginary component emerges for the Floquet Hamiltonian's eigenspectrum (quasienergy). Therefore, we called this method the checking of Floquet Hamiltonian's eigenvalues method. With this result obtained from Yogesh's paper, we are going to investigate using our method of checking for extended unitarity check and find the relationship between the 2 different approaches in tackling the problem.

10.2 Method II: Check for Extended Unitarity

In this section, we are going to use another method to try and obtain the same phase diagram shown in Figure 18 by Yogesh and his team. The method that is going to be used is termed as the method of checking for extended unitarity. Additionally, for this section, we will start to handle Hamiltonians that have unit of energy instead of dimensionless Hamiltonians as in

chapter 6. Before going into the detail of computation, we shall first demonstrate that the Hamiltonian, $H_Y(t)$ studied by Yogesh in his team is actually physically similar (time scaling and rotation) to a slightly modified version of $H_1(t)$ which we call $H_Q(t)$ as follow:

$$H_Q(t) = \hbar\omega[\gamma_Q\sigma_z + i\mu_Q \cos(\omega t)\,\sigma_x] \tag{10.3}$$

We also return the $\hbar\omega$ which was removed in chapter 6 for simplicity back to the Hamiltonian so that it has units of energy again. Furthermore, the sine function in $H_1(t)$ is also being replaced by a cosine function and time-scaled so as to map the Hamiltonian to $H_Y(t)$. Lastly, it also does not take much effort to show that the relationship between $H_Y(t)$ and $H_1(t)$ is in fact just a scaling of time and rotation which are transformations that do not affect the form of the time-dependent Schrödinger equation as shown in Appendix E.

In Yogesh's Paper, the Hamiltonian, $H_Y(t)$ when $N = 2$ is given by equation (10.1). A rotation performed on $H_Q(t)$ by applying $i\sigma_y$ will turn $H_Q(t)$ into the form of $H_Y(t)$ immediately as follow:

$$i\sigma_y H_Q(t) = i\mu_Q\hbar\omega \cos(\omega t)\,\sigma_z - \hbar\omega\gamma_Q\sigma_x \tag{10.4}$$

Comparing equation (10.1) with equation (10.4) we see that

$$J = \omega\gamma_Q \quad \text{and} \quad \gamma_Y = \mu_Q\omega \tag{10.5}$$

Therefore, it is obvious now that the parameters γ and μ which we studied in chapter 6 is being mapped into the terms, J and γ_Y that is used in Yogesh's paper. Since it is now clear that $H_Y(t)$ and $H_Q(t)$ are physically equivalent, a check for extended unitarity on $H_Y(t)$ using parameters $(\frac{\gamma_Y}{J}, \frac{\omega}{J})$ and setting $J = 1$ is performed in Mathematica and a phase diagram that resembles Figure 18 is obtained and shown in Figure 19. The reason why $(\frac{\gamma_Y}{J}, \frac{\omega}{J})$ is being chosen as parameters is because the pair is equivalent to $\left(\frac{\gamma_Y}{J} = \frac{\mu_Q}{\gamma_Q}, \frac{\omega}{J} = \frac{1}{\mu_Q}\right)$ which we had studied earlier on. In other words, the phase diagram obtained in Figure 18 can also be obtained from Figure 3 just by redefining the axis as $\left(\frac{\mu_Q}{\gamma_Q}, \frac{1}{\mu_Q}\right)$.

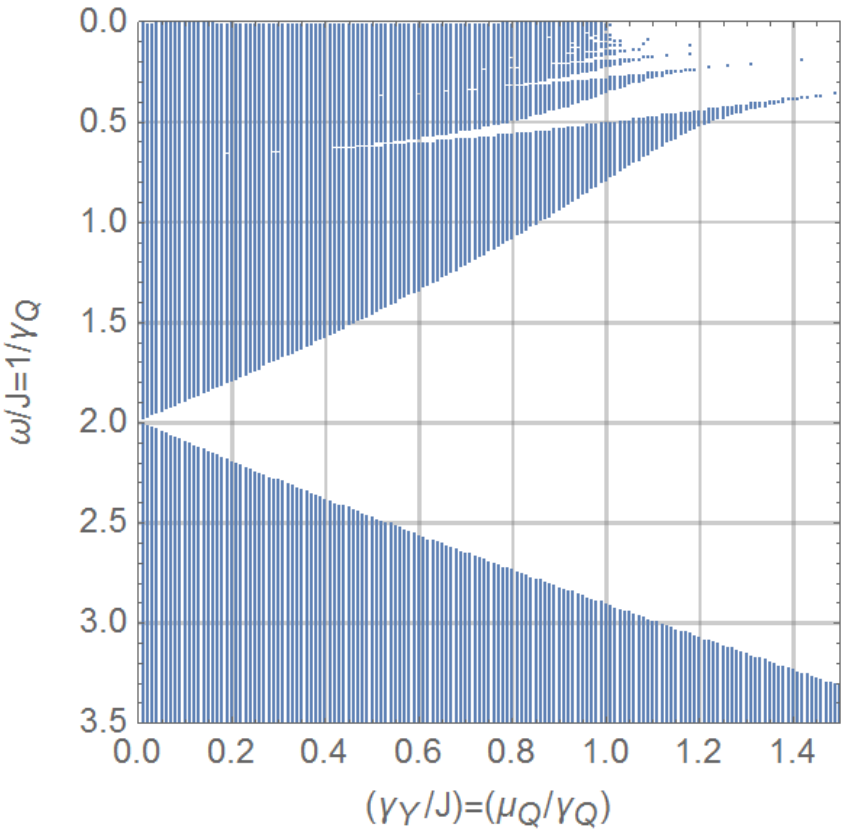

Figure 19 Plot of the phase diagram for $\left(\frac{\omega}{J}=\frac{1}{\mu_Q}\right)$ against $\frac{\gamma_Y}{J}=\frac{\mu_Q}{\gamma_Q}$ for Hamiltonian, $\boldsymbol{H_Y(t)}$ whereby the blue shaded regions are domains where extended unitarity condition is being fulfilled.

Thus, we have successfully reproduced the same phase diagram in Yogesh's paper via checking for extended unitarity for every point, which is why it is being called the method of checking for extended unitarity.

10.3 Discussion

Upon careful analysis as shown above, we see that the phase diagrams obtained using different methods actually resembles each other. However, Figure 18 is being obtained via checking for the eigenspectrum (quasienergies) of the Floquet Hamiltonian, $H_{Y,F}$ for imaginary components. While Figure 19 is obtained from $H_Y(t)$ directly via checking for extended unitarity in the domains: $(\frac{\gamma_Y}{J},\frac{\omega}{J})$. With this, we come to the result that: *Although these 2 methods look different on the surface, it is actually solving the same set of problems. This is because in chapter 4 we understand from equation (4.20) that when the eigenspectrum (quasienergies) of the*

Floquet Hamiltonian are purely real, it ensures that the eigenvalues of the Floquet operator is just a phase factor i.e. fulfill extended unitarity. Therefore, performing such calculations allows us to see that even though it looks as if we are performing 2 different sets of calculation, we are still at the same aim of trying to find out the system domain which allows stabilization of a non-Hermitian system via periodic driving.

However, it must be emphasized that the second method has advantages over the first method because the second method provides us a more efficient way to evaluate the parameters that satisfy extended unitarity condition. This is because, in the first method, an infinite Floquet Hamiltonian needs to be truncated at certain point in order for a computer to evaluate the eigenvalues. However, it is not known beforehand at which point the Floquet Hamiltonian should be truncated in order for us to obtain meaningful results that are accurate and precise. As a result, much time and efforts might be lost in trying to determine the optimal point of truncation to produce a good result. It is undoubtedly good to perform the truncation at the largest possible value of N_f the computer can handle to reduce the amount of information being loss from the infinite Floquet Hamiltonian. However, it might not be feasible because a large amount of time will be required for the computer to evaluate the eigenvalues, with an insignificant improvement in the accuracy of the results.

Additionally, because of not performing truncation in method 2, it makes method 2 a more accurate method because during the evaluation of the parameters, there is no information being lost. Comparing to the former method whereby truncation of the infinite Floquet Hamiltonian is compulsory for numerical calculations to be performed on a computer, we can see some noise in the phase diagram obtained by Yogesh et.al which is being highlighted using a red rectangle shown in Figure 18. Taking a look at the phase diagram obtained via using the method of checking for extended unitarity in Figure 19 we see well defined boundaries clearly without any noises.

In conclusion, from these 2 different types of calculation, it gave us a better insight on the relationship between the quasienergies of the Floquet Hamiltonian and the condition of extended unitarity. Furthermore, it also illustrates that the second method introduced by us is a better and more accurate method because no information is lost during calculation.

Chapter 11

Potential Applications for Study

In the last chapter of the thesis, we are going to discuss some of the potential applications of our study to inspire further research to be done in this field.

11.1 Testing Tool for Perfectness of a Sinusoidal Function

Today, the ability for a function generator to generate as perfect as possible a sinusoidal function is of great importance for obtaining precise and accurate experimental results. Hence, much effort has been devoted to develop function generators so as to help in facilitating the production of nice sinusoidal waveform for use in experimental settings [41]. This is of great importance because certain experiments that involve quantum mechanics are very intrinsic in nature. Any tiny "flaws" can easily lead to a wrong or misleading conclusion for an experiment.

In view of this, we spotted a potential application of our research in checking for the "perfectness" of sinusoidal functions that are being generated by a function generator. This is possible if we were to prepare our system with suitable parameters of (γ, μ) such that it lies on the boundaries between domains which satisfy extended unitarity and domains which do not satisfy extended unitarity in the phase diagram. Upon doing so, we will now make use of the sinusoidal field that is being generated by the function generator to drive the system. If the system remains stable, we conclude that the sinusoidal field generated by the function generator is close to perfect and vice versa.

This can be illustrated using the following example whereby the same Hamiltonian, $H_1(t)$ in chapter 6 is being used but with a small modification: The driving sinusoidal function is being shifted by a small parameter, ϵ.

$$H_5(\epsilon, t) = \begin{pmatrix} \gamma & i(\epsilon + \mu \sin(t)) \\ i(\epsilon + \mu \sin(t)) & -\gamma \end{pmatrix}$$

When $\epsilon = 0.01$, the following phase diagram is being obtained and shown in Figure 20

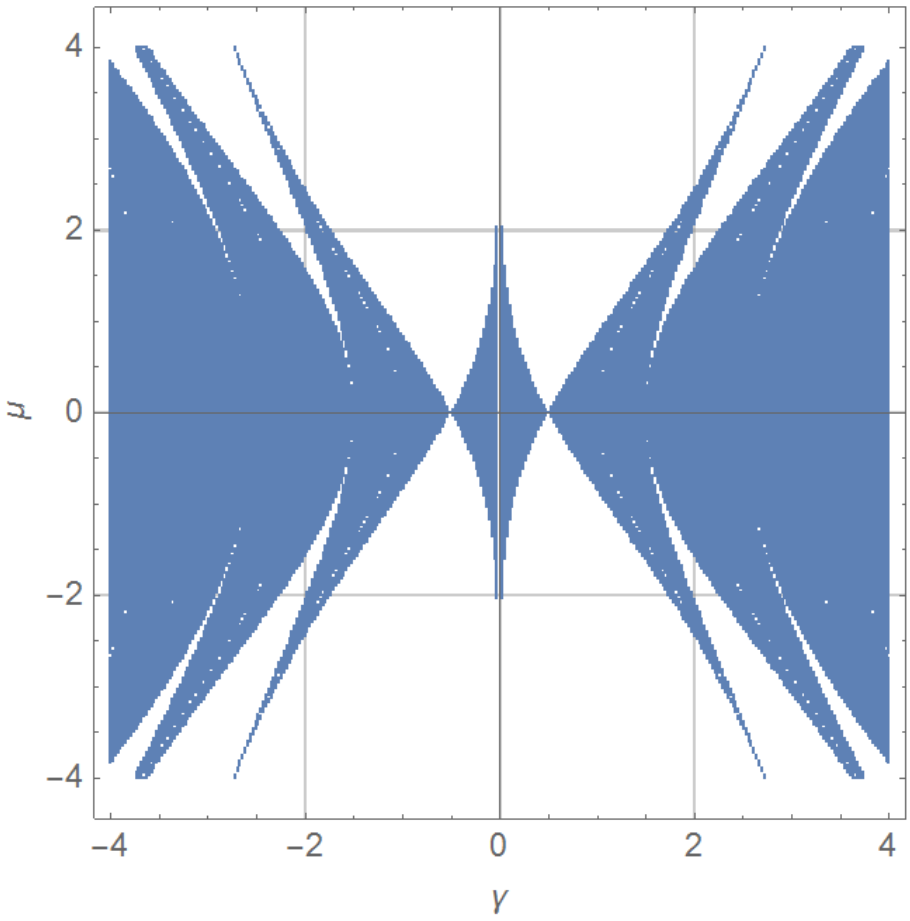

Figure 20 Phase Diagram for parameters $\boldsymbol{\gamma}, \boldsymbol{\mu}$ for Hamiltonian, $\boldsymbol{H_5(t)}$ when $\boldsymbol{\epsilon = 0.01}$. Shaded regions are domains of $\boldsymbol{\gamma}, \boldsymbol{\mu}$ whereby extended unitarity condition is fulfilled.

Upon observing Figure 20 and comparing with Figure 3, we can see that when $\epsilon = 0.01$, some of the domains where extended unitarity used to be present in Figure 3 no longer have this property anymore such as the case of $(\gamma = 0.0001, \mu = 3)$. By performing a population evaluation on this particular point for the case where the Hamiltonian is $H_1(t)$ exactly, we get the following population evolution graph for both states in Figure 21a and 21b. Both figures show that this particular domain of γ and μ fulfills extended unitarity condition because a stable and coherent generalized Rabi oscillation is being observed.

However for the case of $H_5(t)$ when $\epsilon = 0.01$, at $(\gamma = 0.0001, \mu = 3)$, the generalized Rabi oscillation of the state blows up quickly after some period of oscillation as shown in Figure 22a and Figure 22b.

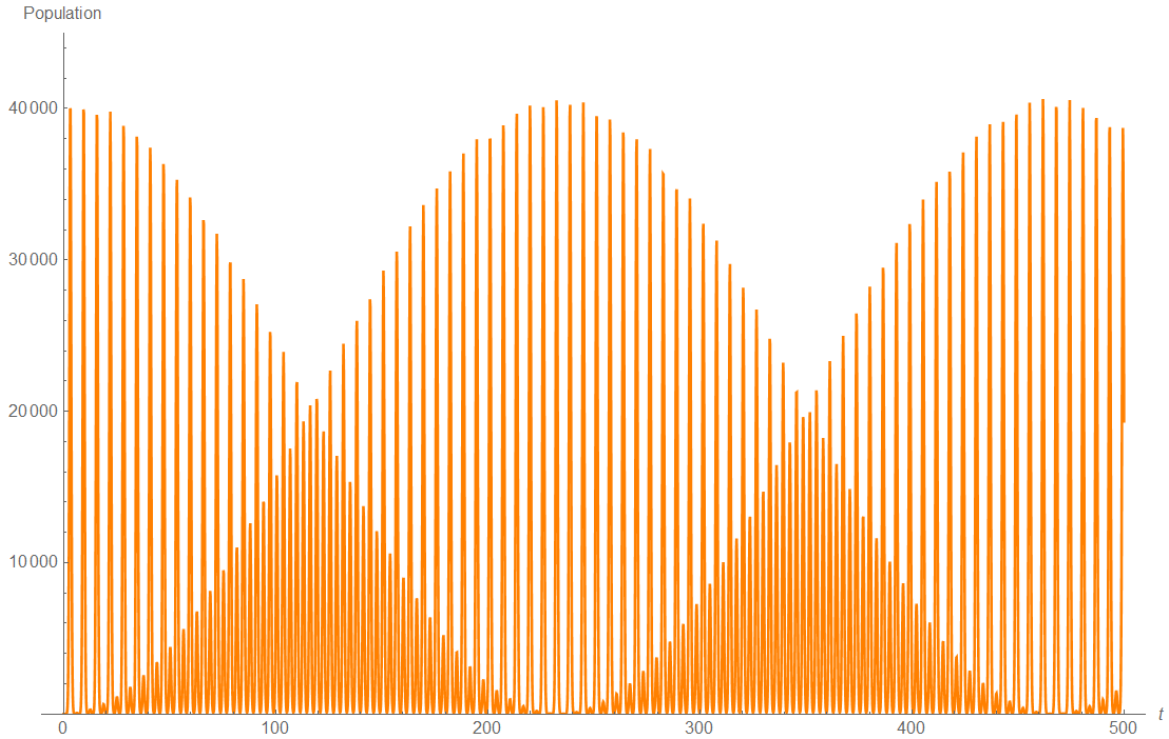

Figure 21a Plot of Generalized Rabi oscillation for Hamiltonian. $\boldsymbol{H_1(t)}$ for $(\boldsymbol{\gamma = 0.0001, \mu = 3})$ via populations of spin up.

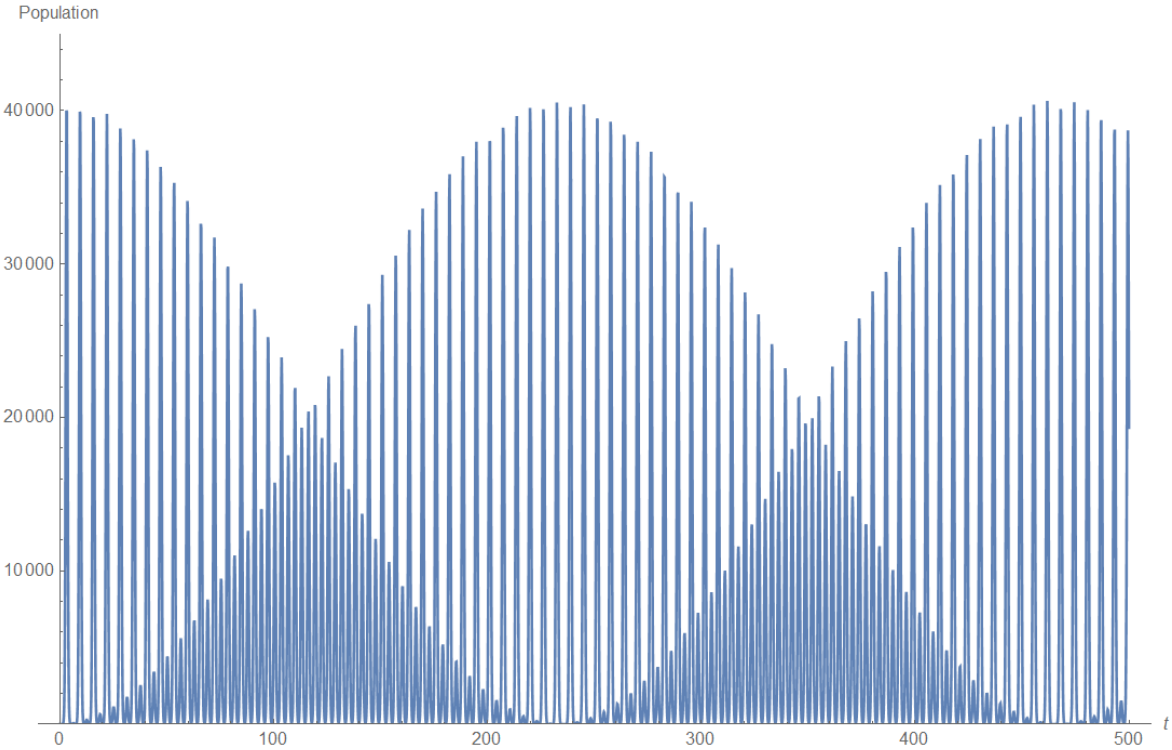

Figure 21b Plot of Generalized Rabi oscillation for Hamiltonian. $H_1(t)$ for $(\gamma = 0.0001, \mu = 3)$ via populations of spin down.

Figure 22a Plot of Generalized Rabi oscillation for Hamiltonian. $\boldsymbol{H_5(t)}$ for $(\boldsymbol{\gamma = 0.0001, \mu = 3, \epsilon = 0.01})$ via populations of spin up.

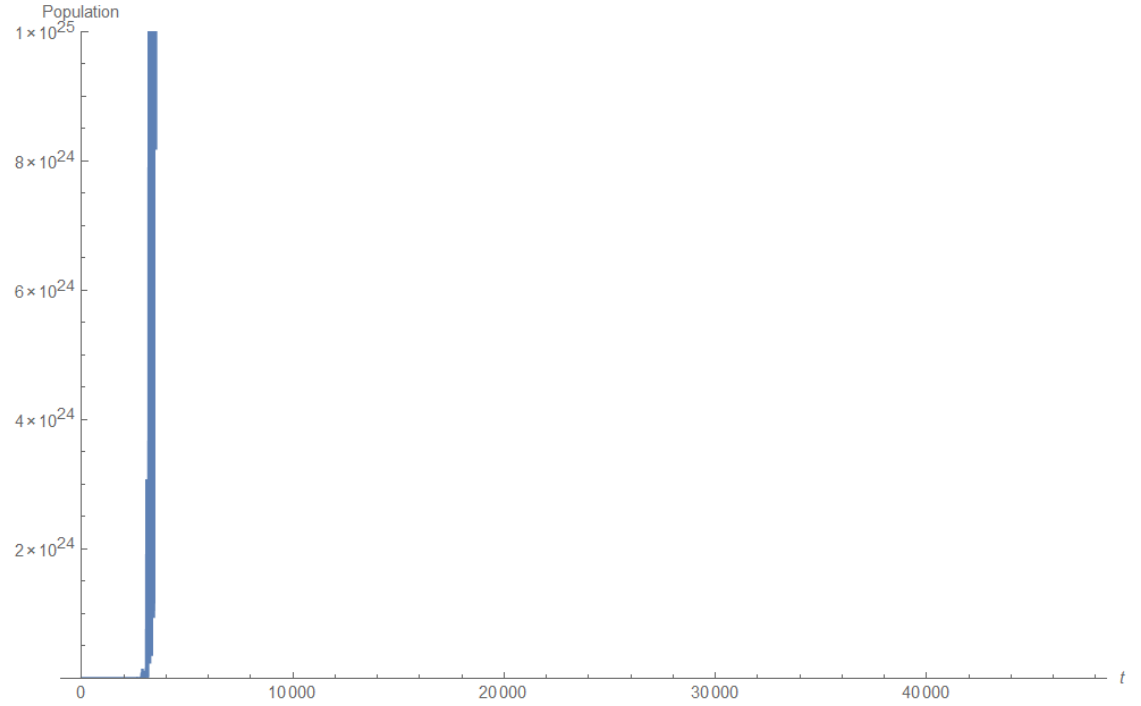

Figure 22b Plot of Generalized Rabi oscillation for Hamiltonian. $H_5(t)$ for $(\gamma = 0.0001, \mu = 3, \epsilon = 0.01)$ via populations of spin down.

Thus, if we were to prepare a system having Hamiltonian $H_1(t)$ with $(\gamma = 0.0001, \mu = 3)$ and drive it using a "sinusoidal function", the system should remain stabilized if the function is indeed sinusoidal. However, if there are some small deviations, it will be picked up by the system by becoming destabilized. This will thus allow us to conclude that the driving function is not perfectly sinusoidal.

With this, we can see that this method can be used as a tool to check for perfectness of the sinusoidal function generated by a function generator before intrinsic experiment is being performed using the generator. This can also be generalized to arbitrary distortion of the sinusoidal function and assist us in testing for any imperfection in the driving sinusoidal function.

11.2 Light Wave Propagation in a Waveguide

As mentioned at the beginning of the thesis, the concept of stabilization of non-Hermitian quantum mechanical system via periodic driving is to date not experimentally verified due to limitation of current technology in preparing quantum mechanical systems with non-Hermitian Hamiltonians [16]. Even if advancement in technology enables us to do so, the introduction of non-Hermitian terms is only an approximation for a decaying system as mentioned by Bender [16]. Furthermore, in various theoretical study on Parity-Time symmetry, we realized that Hermiticity of Hamiltonians is not an absolute condition for real energy eigenspectrum as well [42]. As a result, this extension to the theory of quantum mechanics is still subjected to debate despite having extensive theoretical studies being done due to the lack of strong experimental evidence for verification [14-16, 43, 44].

However, this is not the case for the realm of optics because optical systems with complex refractive indices are realizable with today's technology and are widely used in experiments to verify PT-symmetry in non-Hermitian optical systems. The study being done in this thesis is applicable in the realm of optics because of the close mathematical resemblance between the time-dependent Schrödinger equation and the 2-dimensional Inhomogeneous Paraxial Wave Equation [45]:

$$i\frac{\partial E(x,z)}{\partial z} + \frac{1}{2k}\frac{\partial^2 E(x,z)}{\partial x^2} - V(x,z)E(x,z) = 0$$

where $E(x,z)$ is the electric field of light and $V(x,z)$ is the refractive index of the optical system.

Similar to the mapping that is done in chapter 9 which maps a non-Hermitian periodically driven system into a band structure problem, it is also possible to map a quantum mechanical system to an optical system. This is because electron transport in periodic crystalline potentials and quantum tunneling in periodically driven system can be represented mathematically similar to an effectively controlled light propagation in waveguides via careful periodic modulations. In the case of an optical system, our "periodic driving" is analogous to light passing through a medium with periodic refractive index, making it equivalent to our time-periodic non-Hermitian system as studied in previous chapters [43, 44].

In our study, we focus on stabilizing the system with respect to time. Hence, it becomes a study of under what conditions that the system satisfies extended unitarity conditions i.e. stabilized system. If extended unitarity conditions are not fulfilled, the dynamics of the system either grow exponentially or decay. However, in the optical system, if the "extended unitarity" condition or "pseudo-PT symmetry" coined by Luo et. al. is not fulfilled, it will lead to the time-averaged total intensity of the quasistationary light to grow [44]. In view of this, we can actually control the modulation of the refractive indices in a way such that extended unitarity conditions are no longer satisfied. Making use of these non-extended unitarity domains, the intensity of the light can be made to grow exponentially even for arbitrarily weak gain or loss. This will be a very useful application because it provides us an efficient way to perform beam amplification in optical waveguides via exponentially increasing the intensity of the light.

As the scope of this topic goes beyond the main purpose of this paper, it shall not be discussed in depth here. Interested readers can refer to literature by Luo et.al. for more in depth explanations and derivations [44].

Chapter 12

Summary

Summarizing, the study of stabilizing non-Hermitian Hamiltonian systems is a very interesting one because we can start to appreciate more on the formalism of the basic postulates of quantum mechanics now. From the study of non-Hermitian systems, we have also managed to extend slightly on the theory of quantum mechanics which initially has a postulate that requires a Hamiltonian to be Hermitian. The use of periodic driving to stabilize such open system is also being studied with some smooth and continuous periodic functions and is being proved to be successful in stabilizing open systems at certain parameters. Future research can include more exotic periodic functions such as tangent functions for study to add on to the theoretical background of this topic. Multiple qubit or 3 level systems can also be studied on the basis that a 2 qubit system is being analyzed in this paper and hopefully the concept of extended unitarity can be generalized even further. Additionally, by mapping the non-Hermitian, time periodic system into a band structure problem in chapter 9, it demonstrates the usefulness of this topic in the realm of Solid State Physics. Furthermore, after comparing our method of evaluation with Yogesh et. al., we successfully demonstrated that both methods give optimistic results that agree with each other to a large extent and both methods are able to tackle the same problem successfully. However, our method is superior because of its capability in giving a more accurate result. Lastly, in the final chapter, some further potential applications of our study is being introduced to inspire further research to be done on this field so that this concept can be utilized more in practical settings in the future.

Appendices

Appendix A

Mathematica codes used for evaluation

Mathematica codes are attached at the back of the thesis

Appendix B

Liouville's Formula for a Two-Level Hamiltonian system

Liouville's Formula is given as follows:

$$i\,\frac{\partial}{\partial t}Det[U(t,0)] = Tr[H(t)]Det[U(t,0)]$$

In cases whereby $Tr[H(t)] = 0$, the Liouville's Formula becomes:

$$i\,\frac{\partial}{\partial t}Det[U(t,0)] = 0$$

$$\Rightarrow \quad \frac{\partial}{\partial t}\{Det[U(t,0)]\} = 0$$

$$\Rightarrow \quad \int_0^t d\{Det[U(t,0)]\} = \int_0^t 0\,dt$$

$$Det[U(t,0)] - Det[U(0,0)] = 0$$

Since the initial condition is given as $U(0,0) = I$, and $Det[I] = 1$,

$$Det[U(t,0)] = 1 \tag{B1}$$

Furthermore, if $U(t,0)$ is a diagonal matrix, the eigenvalues of $U(t,0)$ will be the diagonal terms.

If $U(t,0)$ is not diagonalized, it can be diagonalized with the use of a similarity transformation, S as shown below.

$$U(t,0) = SDS^{-1}$$

From linear algebra, we know that

$$Det[U(t,0)] = Det[S]Det[D]Det[S^{-1}]$$

$$\Rightarrow \quad Det[U(t,0)] = Det[S]Det[D]\left(\frac{1}{Det[s]}\right)$$

$$Det[U(t,0)] = Det[D]$$

Combining with (B1), we have the following:

$$Det[U(t,0)] = Det[D] = 1$$

In the case of a two-level Hamiltonian being handled, we can see explicitly that the 2 eigenvalues of the evolution operator, $U(t,0)$ must be a complex conjugate of one another.

$$\therefore U(t,0) = \begin{pmatrix} e^{i\beta_1} & 0 \\ 0 & e^{i\beta_2} \end{pmatrix} = \begin{pmatrix} e^{i\beta} & 0 \\ 0 & e^{-i\beta} \end{pmatrix}$$

Therefore, eigenvalues of $U(t,0)$ can be written as $e^{\pm i\beta}$, where β is a real number.

Appendix C

Dress-State Picture

Matrix notation of the time-dependent Schrödinger equation for the spin $\frac{1}{2}$ system in a magnetic field is shown as follow:

$$i\hbar\frac{\partial}{\partial t}\begin{pmatrix}c_1(t)\\c_2(t)\end{pmatrix}=\begin{pmatrix}-\frac{\hbar\omega_0}{2} & \frac{\hbar\Omega}{2}e^{i\omega t}\\ \frac{\hbar\Omega}{2}e^{-i\omega t} & \frac{\hbar\omega_0}{2}\end{pmatrix}\begin{pmatrix}c_1(t)\\c_2(t)\end{pmatrix}$$

In equation form, the above expression becomes:

$$i\dot{c_1}=-\left(\frac{\omega_0}{2}\right)c_1+\frac{\Omega}{2}e^{i\omega t}c_2 \tag{C1}$$

$$i\dot{c_2}=\frac{\Omega}{2}e^{-i\omega t}c_1+\frac{\omega_0}{2}c_2 \tag{C2}$$

Upon doing a change of variable as follow:

$$\tilde{c}_1=e^{i\omega t}c_1 \qquad \text{and} \qquad \tilde{c}_2=c_2$$

We can turn (C1) and (C2) into

$$i\dot{\tilde{c}}_1=\left(\omega-\frac{\omega_0}{2}\right)\tilde{c}_1+\frac{\Omega}{2}\tilde{c}_2 \tag{C3}$$

$$i\dot{\tilde{c}}_2=\frac{\Omega}{2}\tilde{c}_1+\frac{\omega_0}{2}\tilde{c}_2 \tag{C4}$$

Finally, we recast (C3) and (C4) into matrix form, we get

$$i\hbar\frac{\partial}{\partial t}\begin{pmatrix}\widetilde{c_1}(t)\\\widetilde{c_2}(t)\end{pmatrix}=\hbar\begin{pmatrix}\omega-\frac{\omega_0}{2} & \frac{\Omega}{2}\\ \frac{\Omega}{2} & \frac{\omega_0}{2}\end{pmatrix}\begin{pmatrix}\widetilde{c_1}(t)\\\widetilde{c_2}(t)\end{pmatrix}$$

A *Dress-State Picture* where the Hamiltonian now is time-independent.

Appendix D

Mathematical derivation to obtain equation (9.1)

$$i\dot{u}_0 + i\dot{u}_3 = au_0 + au_3 + ibu_1 - bu_2 \quad \text{(D1)}$$

$$i\dot{u}_1 + \dot{u}_2 = au_1 - iau_2 + ibu_0 - ibu_3 \quad \text{(D2)}$$

$$i\dot{u}_1 - \dot{u}_2 = ibu_0 + ibu_3 - au_1 - iau_2 \quad \text{(D3)}$$

$$i\dot{u}_0 - i\dot{u}_3 = ibu_1 + bu_2 - au_0 + au_3 \quad \text{(D4)}$$

To get $\dot{u}_0$, we perform (D1) + (D4),

$$2\dot{u}_0 i = 2ibu_1 + 2au_3$$

$$\Rightarrow \quad \dot{u}_0 = bu_1 - iau_3$$

To get $\dot{u}_1$, we perform (D2) + (D3),

$$2\dot{u}_1 i = 2ibu_0 - 2iau_2$$

$$\Rightarrow \quad \dot{u}_1 = bu_0 - au_2$$

To get $\dot{u}_2$, we perform (D2) - (D3),

$$2\dot{u}_2 = 2au_1 - 2ibu_3$$

$$\Rightarrow \quad \dot{u}_2 = au_1 - ibu_3$$

To get $\dot{u}_3$, we perform (D1) - (D4),

$$2\dot{u}_3 i = 2au_0 - 2bu_2$$

$$\Rightarrow \quad \dot{u}_3 = -iau_0 + ibu_2$$

Combining them together, we get equation (9.1) as follow:

$$\begin{cases} \dot{u}_0(t) = b(t)u_1(t) - iau_3(t) \\ \dot{u}_1(t) = b(t)u_0(t) - au_2(t) \\ \dot{u}_2(t) = au_1(t) - ib(t)u_3(t) \\ \dot{u}_3(t) = -iau_0(t) + ib(t)u_2(t) \end{cases}$$

Appendix E

To prove that the relationship between $H_Q(t)$ and $H_1(t)$ is just a scaling in time and it does not affect the form of the time-dependent Schrödinger equation, we suppose $H = H(t)$ and using the time-dependent Schrödinger equation

$$i\hbar\frac{\partial}{\partial t}|\Psi(t)\rangle = H(t)|\Psi(t)\rangle$$

Together with the definition of time-evolution operator, $U(t,0)$,

$$|\Psi(t)\rangle = U(t,0)|\Psi(0)\rangle$$

Suppose we let $t = \alpha t'$ and further define $H(\alpha t') \equiv \frac{1}{\alpha}H'(t')$ for reasons that will be clear later, we get:

$$H(t) = H(\alpha t') \equiv \frac{1}{\alpha}H'(t')$$

As the Hamiltonian of concern is periodic, $H(t) = H(t+T)$, we can make use of the definition above to rewrite the system as follow:

$$H(t) = H(t+T)$$
$$\Rightarrow \quad H(\alpha t') = H(\alpha t' + \alpha T')$$
$$\Rightarrow \quad H(\alpha t') = H\big(\alpha(t'+T')\big)$$
$$\Rightarrow \quad \frac{1}{\alpha}H'(t') = \frac{1}{\alpha}H'(t'+T')$$
$$\therefore \quad H'(t') = H'(t'+T')$$

From the above, we see that scaling time does not affect the periodic structure of the originally periodic Hamiltonian.

Going on, we evaluate the time evolution operator, $U(t,0)$ to see if there is any change in form of the time dependent Schrödinger equation as follow:

$$i\hbar\frac{\partial}{\partial t}|\Psi(t)\rangle = H(t)|\Psi(t)\rangle$$
$$\Rightarrow \quad i\hbar\frac{\partial}{\partial t}[U(t,0)|\Psi(0)\rangle] = H(t)U(t,0)|\Psi(0)\rangle$$
$$\Rightarrow \quad i\hbar\frac{\partial U(t,0)}{\partial t} = H(t)U(t,0)$$
$$\Rightarrow \quad i\hbar\frac{\partial t'}{\partial t}\frac{\partial U(\alpha t',0)}{\partial t'} = \frac{1}{\alpha}H'(t')U(\alpha t',0)$$

$$\Rightarrow \qquad i\hbar\frac{1}{\alpha}\frac{\partial}{\partial t'}\,U(\alpha t',0)=\frac{1}{\alpha}H'(t')U(\alpha t',0)$$

$$\therefore \qquad i\hbar\frac{\partial}{\partial t'}\,U(\alpha t',0)=H'(t')U(\alpha t',0)$$

Therefore this helps us come to the conclusion of defining the time evolution operator, $U(t,0)$ after scaling with time as:

$$U'(t',0)=U(\alpha t',0)$$

Finally, we arrived at $i\hbar\frac{\partial}{\partial t'}U'(t',0)=H'(t')U'(t',0)$ and conclude that the rescaling does not change the form of the time dependent Schrödinger equation at all. Therefore, the use of the standard time dependent Schrödinger equation in chapter 10 for the time being scaled by ω is still legitimate.

Bibliography

[1] Morton M.Sternheim and James F. Walker, Phys. Rev. C **6**, 114 (1972).

[2] C Figueira de Morisson Faria and A Fring, J. Phys. A: Math. Gen. **39** (2006) 9269–9289.

[3] Q.-h.Wang, Int. J. Theor. Phys, **50**, 1005-1011 (2011).

[4] J. B. Gong and Q.-h. Wang, J. Phys. A **46**, 485302 (2013).

[5] J. B. Gong and Q.-h. Wang, Stabilizing Non-Hermitian Systems by Periodic Driving (2014) (arXiv:1412.3549).

[6] M. Znojil, Phys. Rev. A **82**, 052113 (2010).

[7] M. Znojil, Phys. Lett. A **375**, 3435 (2011).

[8] O. Bendix, R. Fleischmann, T. Kottos, and B. Shapiro, Phys. Rev. Lett. **103**, 030402 (2009).

[9] L. Jin and Z. Song, Phys. Rev. A **80**, 052107 (2009).

[10] Y. N. Joglekar, D. Scott, M. Babbey, and A. Saxena, Phys. Rev. A **82**, 030103(R) (2010).

[11] Y. N. Joglekar and A. Saxena, Phys. Rev. A **83**, 050101(R) (2011).

[12] D. D. Scott and Y. N. Joglekar, Phys. Rev. A **83**, 050102(R) (2011).

[13] G. Della Valle and S. Longhi, Phys. Rev. A **87**, 022119 (2013).

[14] C. M. Bender and S. Boettcher, Phys. Rev. Lett. **80**, 5243 (1998).

[15] C. M. Bender, D. C. Brody, and H. F. Jones, Phys. Rev. Lett. **89**, 270401 (2002).

[16] C. M. Bender, Rep. Prog. Phys. **70**, 947 (2007).

[17] M. V. Berry, J. Opt. **13**, 115701 (2011).

[18] S. Longhi, Phys. Rev. Lett. **103**, 123601 (2009).

[19] C. T. West, T. Kottos, and T. Prosen, Phys. Rev. Lett. **104**, 054102 (2010).

[20] A. Mostafazadeh, J. Math. Phys. **43**, 205 (2002); ibid 43, 2814 (2002).

[21] G. Della Valle, M. Ornigotti, E. Cianci, V. Foglietti, P. Laporta, and S. Longhi, Phys. Rev. Lett. **98**, 263601 (2007).

[22] A. Szameit, Y. V. Kartashov, F. Dreisow, M. Heinrich, T. Pertsch, S. Nolte, A. Tunnermann, V. A. Vysloukh, F. Lederer, and L. Torner, Phys. Rev. Lett. **102**, 153901 (2009).

[23] X. Luo, J. Huang, H. Zhong, X. Q. Xie, Y. S. Kivshar, and C. Lee, Phys. Rev. Lett. **110**, 243902 (2013).

[24] S. Nixon and J.-k. Yang, Light propagation in periodically modulated complex waveguides (2014) (arXiv:1412.6113).

[25] Nouredine Zettili, Quantum Mechanics Concepts and Applications, 2nd ed., p.165-167;573-574 (2009).

[26] MIT Open Courseware Lecture Notes: Time Evolution in Quantum Mechanics *(Available for download at http://ocw.mit.edu/courses/nuclear-engineering/22-02-introduction-to-applied-nuclear-physics-spring-2012/lecture-notes/MIT22_02S12_lec_ch6.pdf).*

[27] M. Born: Quantenmechanik der Stoßvorgange. Z. Phys. 38, 803-827 (1926).

[28] J.H. Shirley, Solution of the Schrodinger equation with a Hamiltonian periodic in time, Phys. Rev. 138, B 979 (1965). doi:10.1103/PhysRev.138.B979.

[29] D. Zwillinger, Handbook of Differential Equations, p.450 (2014).

[30] K. Fujii, (2014) Introduction to the Rotating Wave Approximation (RWA): Two Coherent Oscillations (arXiv:1301.3585v2).

[31] C. M. Bender Invited paper in Contemporary Physics **46**, 277 (2005) (arXiv: quant-ph/0501052).

[32] M. E. Fisher, Phys. Rev. Lett. **40**, 1610 (1978).

[33] J. L. Cardy, ibid. **54**, 1345 (1985).

[34] J. L. Cardy and G. Mussardo, Phys. Lett. B **225**, 275 (1989).

[35] A. B. Zamolodchikov, Nucl. Phys. B **348**, 619 (1991).

[36] C. F. M. Faria and A. Fring, ISSN 1054-660X, Laser Physics, (2007), Vol 17, No. 4, p. 424-437.

[37] J. B. Gong and Q.-h. Wang, Phys. Rev. A. **82**, 012103 (2010).

[38] Stephen H. Friedberg, Arnold J. Insel and Lawrence E. Spence, Linear Algebra, 4th ed., p.482 (2003).

[39] Yogesh N. Joglekar, Rahul Marathe, P. Duranandini and Rajeev K. Pathak, Phys. Rev. A. **90**, 040101(R) (2014).

[40] U. Peskin and N. Moiseyeev, J. Chem. Phys. **99**,4590 (1993).

[41] Karrenberg, U., An Interactive Multimedia Introduction to Signal Processing, 2007, XII, p. 33-64.

[42] Barton G 1963 *Introduction to Advanced Field Theory* (New York: Wiley) chapter 12.

[43] K. G. Makris, R. El-Ganainy, and D. N. Christodoulides, PRL **100,** 103904 (2008).

[44] Xiaobing Luo, Jiahao Huang, Honghua Zhong, Xizhou Qin, Qiongtao Xie, Yuri S. Kivshar and Chaohong Lee, PRL, **110**, 243902 (2013).

[45] S. Longhi, Laser Photonics Rev. **3**, 243 (2009).

[46] Ya. B. Zeldovitch, Sov. Phys. JETP **24**,1006 (1967); V. I. Ritus, Sov. Phys. JETP **24**, 1041 (1967).

[47] G. Floquet, Ann. de l'Ecole Norm. Sup. **12**, 47 (1883);

[48] E. L. Ince, *Ordinary Differential Equations* (Dover Publ., New York, 1956);

[49] W. Magnus and S. Winkler, *Hill's Equation* (Dover Publ., New York, 1979).

[50] H. Sambe, Phys. Rev. A **7**, 2203 (1973).